Portable Metal Shrapnel Detector for Removal of Shrapnel inside Human Body

Submitted By

AMBILI A R

for the award of the degree

of

MASTER OF TECHNOLOGY

Under the guidance of

Dr. Boby George

DEPARTMENT OF ELECTRICAL ENGINEERING
INDIAN INSTITUTE OF TECHNOLOGY MADRAS
May 2014

THESIS CERTIFICATE

This is to certify that the thesis titled " **PORTABLE METAL SHRAPNEL DETECTOR FOR REMOVAL OF SHRAPNEL INSIDE HUMAN BODY** ", submitted by **Mrs Ambili A R** , to the Indian Institute of Technology Madras, Chennai for the award of the degree of **Master of Technology**, is a bonafide record of research work done by her under my supervision. The contents of this thesis, in full or a part has not been submitted to any other Institute or University for the award of any degree or diploma.

Dr. Boby George
Research Guide
Asst.Professor
Dept. of Electrical Engineering
IIT-Madras, Chennai-600036

Place: Chennai
Date: 22 May 2014

ACKNOWLEDGEMENTS

ABSTRACT

Keywords:- Shrapnel, Microcontroller, Inductive Proximity Sensor (IPS), ADC

Sophisticated and portable medical devices are enabling advances in medical field with their reduced size and cost. As portability becomes a growing trend in medical products, manufacturers are seeking technologies that reduce the design complexity and time in developing the finished product. The "**PORTABLE METAL SHRAPNEL DETECTOR FOR REMOVAL OF SHRAPNEL INSIDE HUMAN BODY**" is developed to locate the metal shrapnel inside the human body which is based on a microcontroller Atmel ATXMEGA128A1. Its main features are: a Low power, high performance 8/16-bit AVR microcontroller featuring 256KB self-programming flash program memory, 4-channel DMA controller, 8-channel event system, and up to 32 MIPS throughput at 32MHz. Microcontrollers (MCUs) provide the right combination of programmability, cost, performance, and power consumption.

The project is highly relevant in the medical scenarios where injuries those caused by weapons or bomb blasts may contain material like steel, aluminum, copper etc .To retrieve the foreign bodies from the soft tissues , doctors nowadays rely on imaging systems like CT, MRI and X-ray. The retrieval seems somewhat difficult when these are penetrated deeply into the tissues. So sometimes its untraceable during surgery. The success of removal of shrapnel depends on the doctor's skill to trace and locate the shrapnel. This necessitates an online tool for locating the metal shrapnel inside the body which is detailed in the project. The details about the sensor and the controller are given in the following chapters. To detect the presence of metals in human bodies during injuries, a new inductive proximity sensor (IPS) was developed. Because of the use of

differential sensing scheme, and the particular design of former, the detection depth is increased. Since the low amplitude and high frequency signals present on the sensor output, it seems difficult to process the output with simple electronic circuitry .And to make a compact, cost-effective portable sensor and easy processing of the sensor output, according to the requirement, the sensor output is designed around the microcontroller. Atmel ATXMEGA is chosen because of its high speed ADC and high CPU frequency of 32MHz

LIST OF FIGURES

ABBREVIATIONS

ADC	Analog to Digital Converter
BFO	Beat Frequency Oscillator
CT	Computer Tomography
CPU	Central Processing Unit
CMP	Compare
DMA	Direct Memory Access
DAC	Digital to Analog Converter
DC	Direct Current
EEPROM	Electrically Erasable Program Read Only Memory
IPS	Inductive Proximity Sensor
PER	Period
PI	Pulse Induction
LED	Light Emitting Diode
MOSFET	Metal Oxide Semiconductor Field Effect Transistor
MSPS	Mega Samples Per Second
RAM	Random Access Memory
SRAM	Static Random Access Memory

TABLES

SYMBOLS

B   Magnetic Field Intensity

μ   Permeability of free space

n   Number of Turns of the Coil

V_{os} Offset Voltage

V_d Differential Voltage

I Current through the coil

V_p Peak Voltage

A_{gain} Gain without considering Offset

A_{offset} Gain with offset

μs   Microseconds

ms   Milliseconds

Z_s Impedance between secondary of sensing and dummy coil

Z_p Impedance between primary of sensing and dummy coil

Z_e Impedance between leads

CHAPTER 1
INTRODUCTION

1.1 PURPOSE OF THE PROJECT

Microcontrollers have wide variety of applications in biomedical engineering. The aim of this project is to develop a microcontroller based metal shrapnel detector to locate the metal shrapnel inside the human body. Wounds, especially those caused by weapons or bomb blast, may contain various materials such as metal, glass etc. But most of these injuries may contain metals like aluminum, steel and copper [1]. Retrieval of these metals inside the body may be quite challenging depending on many factors such as the size of the object, the location, and the surrounding anatomical structures. Imaging Techniques is very important in deciding upon the surgical approach. Current imaging techniques which are employed for detecting foreign bodies include X-ray, computer tomography (CT), magnetic resonance imaging (MRI) and ultrasound imaging [2]. A CT image showing shrapnel inside the body of a blast victim and typical shrapnel materials observed in such incidents are shown in figure 1.1 [3]. Here sometimes even if the shrapnel is clearly visible in the images, it may have penetrated deeply into the tissues. So the recovery of these depends on the doctor's skill. This made a clinical requirement for online sensing tool which guide the doctors to accurately locate the shrapnel and retrieve it easily.
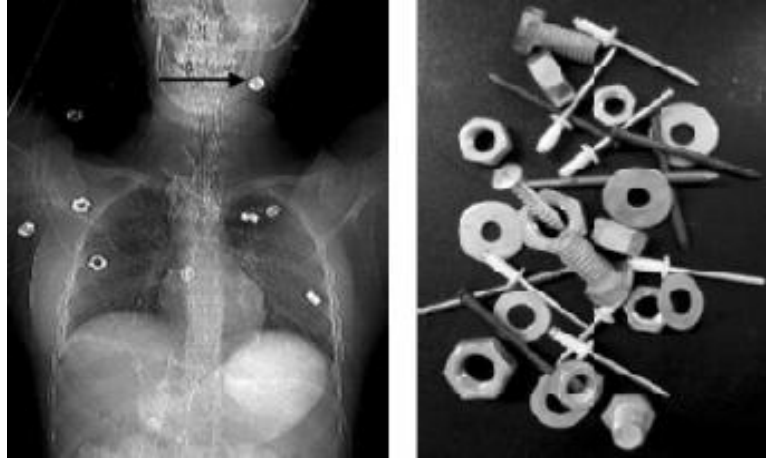
Fig 1.1 CT scan Image of Shrapnel inside a bomb blast victim and object got from victim [3]

Eddy current sensors are mostly used as metal detectors. Here the main constraint is on the size of the tool. The size of the tool should be very small since the diameters should satisfy the surgical standards. As the diameter of the tool is small, the detection depth also should be small [4]. So inductive proximity along with differential sensing technology, is used as the basement for the particular IPS (Inductive Proximity Sensor). The high sampling rate and small amplitude of the sensor output urges the need for using a microcontroller to process the output signal. Here Atmel ATXMEGA128A1 microcontroller is used to process the sensor output. The central part of the entire system is microcontroller, which is used for producing control signals to the entire circuit.

1.2 ORGANIZATION OF THE THESIS

The remainder of the thesis is logically divided into the following chapters. Chapter2 explains the background of the older technologies and the differential sensing scheme which is the back bone of the new IPS (Inductive Proximity Sensor). The main

features of the new IPS and detailed descriptions of the new design is clearly described in chapter 3.The main data acquisition and processing component Atmel ATXMEGA 128A1 microcontroller is explained in chapter 4. Also, the program flow is explained with the aid of flowcharts in chapter 4.Chapter 5 describes the tests and experiments performed in order to verify the operation of the instrument and to study the important characteristics such as sensitivity and range of the device. Chapter 6 gives a summary of the thesis, conclusions and suggestions for future work.

CHAPTER 2

METHODS FOR DETECTING METALIC OBJECTS

2.1 BACKGROUND

Metal detectors are widely used in various industrial applications. They are based mostly on eddy current sensing. Metal detector use one of the three technologies.

2.1 .1 Very Low Frequency (VLF)

VLF metal detector relies on a phenomenon known as phase shifting [5]. Phase shifting is the difference in timing between the transmitter coil's frequency and the frequency of the target object. An object with high inductance is going to have a larger phase shift, because it takes longer to alter its magnetic field. An object with high resistance is going to have a smaller phase shift. Since most metals vary in both inductance and resistance, a VLF metal detector examines the amount of phase shift, using a pair of electronic circuits called phase demodulators, and compares it with the average for a particular type of metal.
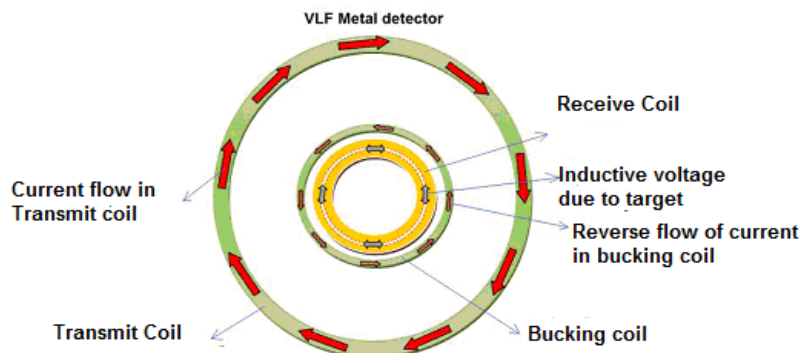
Fig 2.1 VLF Detector [5]

2.1.2 Pulse Induction (PI)

A less common form of metal detector is based on pulse induction (PI) [5]. Unlike VLF, PI uses a single coil as both transmitter and receiver, or they may have two or even three coils working together. This technology sends powerful, short bursts (pulses) of current through a coil of wire. Each pulse generates a brief magnetic field. When the pulse ends, the magnetic field reverses polarity and collapses very suddenly, resulting in a sharp electrical spike. This spike lasts a few microseconds (millionths of a second) and causes another current to run through the coil. This current is called the reflected pulse and is extremely short lasting only about 30 microseconds. Another pulse is then sent and the process repeats. If the metal detector is over a metal object, the pulse creates an opposite magnetic field in the object. When the pulse's magnetic field collapses, causing the reflected pulse the magnetic field of the object makes it take longer for the reflected pulse to completely disappear. A sampling circuit in the metal detector is set to monitor the length of the reflected pulse. By comparing it to the expected length, if the decay of the reflected pulse takes more than a few microseconds longer than normal, there is probably a metal object interfering with it.
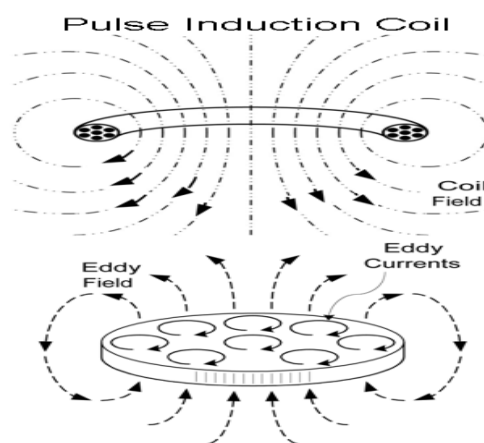
Fig 2.2 Eddy current Generation in a Pulse Induction Coil [5]

2.1.3 BFO Technology

The most basic way to detect metal uses a technology called beat frequency oscillator (BFO). In a BFO system, there are two coils of wire. One large coil is in the search head, and a smaller coil is located inside the control box. Each coil is connected to an oscillator that generates thousands of pulses of current per second. The frequency of these pulses is slightly offset between the two coils. As the pulses travel through each coil, the coil generates radio waves. A tiny receiver within the control box picks up the radio waves and creates an audible series of tones (beats) based on the difference between the frequencies. If the coil in the search head passes over a metal object, the magnetic field caused by the current flowing through the coil creates a magnetic field around the object. The object's magnetic field interferes with the frequency of the radio waves generated by the search-head coil. As the frequency deviates from the frequency of the coil in the control box, the audible beats change in duration and tone.

The targets induced field is very small in the presence of a much larger transmit field. So a second coil can be placed such that it inductively couples with the transmit coil. By careful placement of the secondary coil, the effect of the transmit field can be reduced. If the coils are placed in a null of the transmit field, there won't be any coupling. In such a case the coils are said to be inductively balanced. This is called induction balance. The main design constraint for the sensor in this application is its size. The size of the sensor should satisfy the requirement of a surgical tool. The size is proportional to the induced transmit field .So the detection depth is also get reduced. Therefore to increase the detection depth, the differential sensing method is adopted in new IPS sensor.
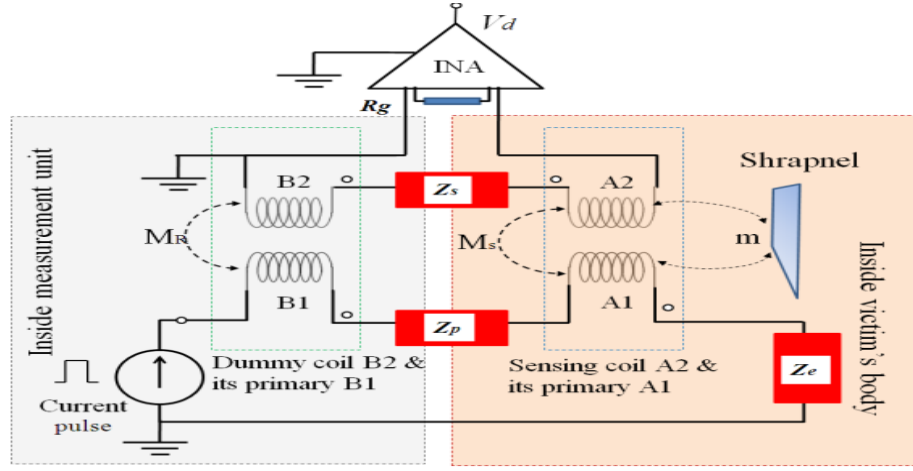
Fig 2.3 Equivalent Circuit of the Differential Measurement Scheme [6]

A miniature IPS [6] which uses differential sensing is shown below in figure 2.3. IPS has sensing coil A2 and a dummy coil B1. When current pulse is given, it will generate a magnetic field in A1 and B1.This magnetic field is inductively coupled into the secondary and this difference voltage is processed by the differential amplifier. The main disadvantages of the circuit are as follows:

1) Due to some geometrical mismatch between coils, there is a chance of offset voltage, even in the absence of target. This offset voltage is indicated as V_{os} throughout the discussions.

2) There is a parasitic impedance Z_s (impedance between secondary of sensing coil and dummy coil), Z_p (impedance between primary of sensing coil and dummy coil) and Z_e (impedance of exciting leads).

2.2 PROPOSED METHOD

New inductive proximity sensor [IPS] [6] is based on differential sensing scheme. It has an air cored coil. Close-in excitation is preferred because continuous current can

make harm to the body. The main change made is on the former design. When a metal piece exists around this proposed sensor, an eddy current is induced due to the magnetic field generated by the transmitting coil. The magnetic field generated by this eddy current is received by a sensing coil which in turn produces a differential output voltage. But the output of the sensing probe is of low amplitude and also exhibits a faster rise and decay. It seems to be difficult to be processed by the usual electronic circuit. So to make a compact and cost effective circuit, the microcontroller was chosen to process the output. The maximum frequency component in the sensor output is found to be 100 KHz. So the minimum sampling rate required to process the sensor voltage is fixed at 1MSPS (Nyquist Criteria). To meet that design requirement, microcontroller ATMEL ATXMEGA128A1 was selected. The enhanced features of ATXMEGA128A1U proved that it was an adequate selection for this application. The evaluation board contains an inbuilt speaker, which is used to generate a sound corresponding to the processed voltage. The heart of the entire instrument, IPS will be discussed in Chapter3 and the brain of the circuit is described in Chapter 4.

CHAPTER 3

DESIGN AND DEVELOPMENT OF THE PORTABLE

METAL SHRAPNEL DETECTOR INSIDE HUMAN BODY

The aim of the project is to develop an online sensing probe which gives real time information about the location of the metal shrapnel inside the body. This tool should be capable of inserting into the body. So the size should be small. The entire system is designed to help the doctor's to locate the shrapnel inside the body during surgery. So it should be lightweight and portable. So microcontrollers are selected that can also reduces the design complexities and time in developing the finished products.

The maximum frequency component in the new IPS sensor output is found to be 100 KHz. So the minimum sampling rate required to process the sensor voltage is fixed at 1MSPS (Nyquist Criteria). To meet that design requirement, microcontroller ATMEL ATXMEGA128A1 was selected. The enhanced features of ATXMEGA128A1U proved that it was an adequate selection for this application. The evaluation board contains an inbuilt speaker, which is used to generate a sound corresponding to the processed voltage. A detailed discussion about new IPS sensor and microcontroller ATXMEGA 128A1 is given in the following chapters. A conceptual diagram of the instrument [6] during surgery is displayed in Fig 3.1
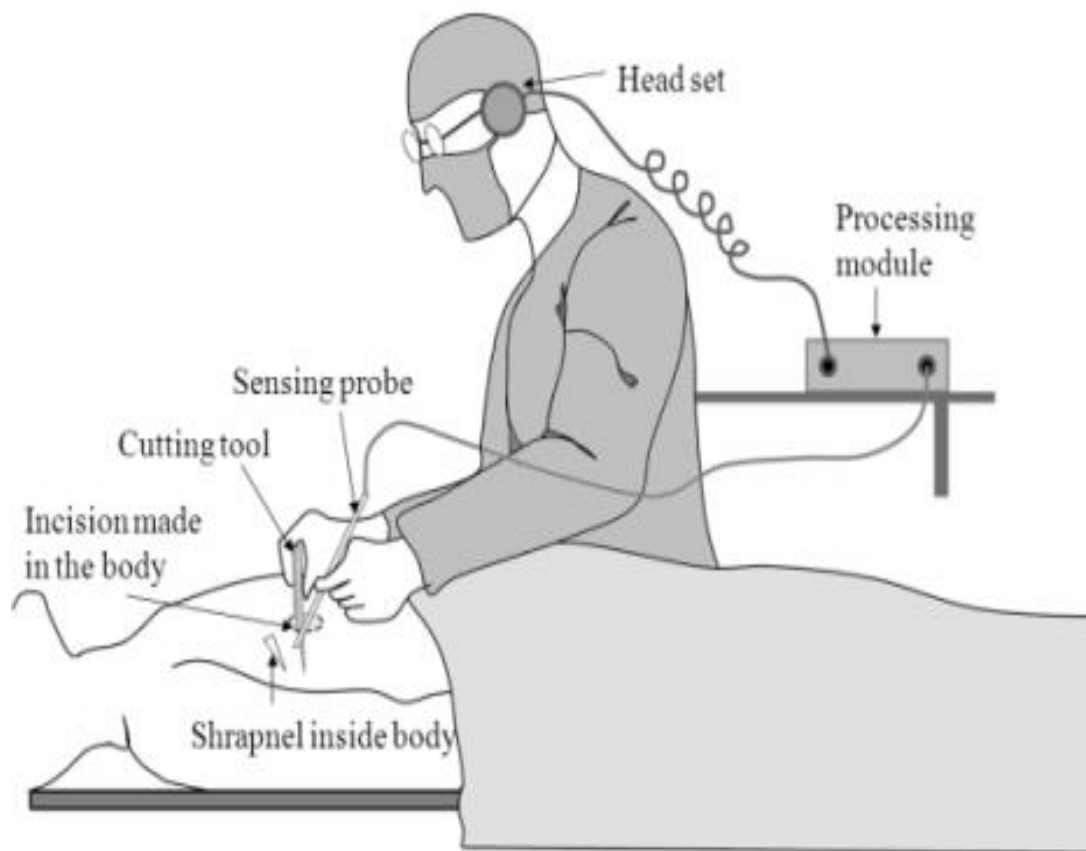
Fig 3.1 Conceptual System for the Measurement System During Surgery[6]

3.2 BLOCK DIAGRAM
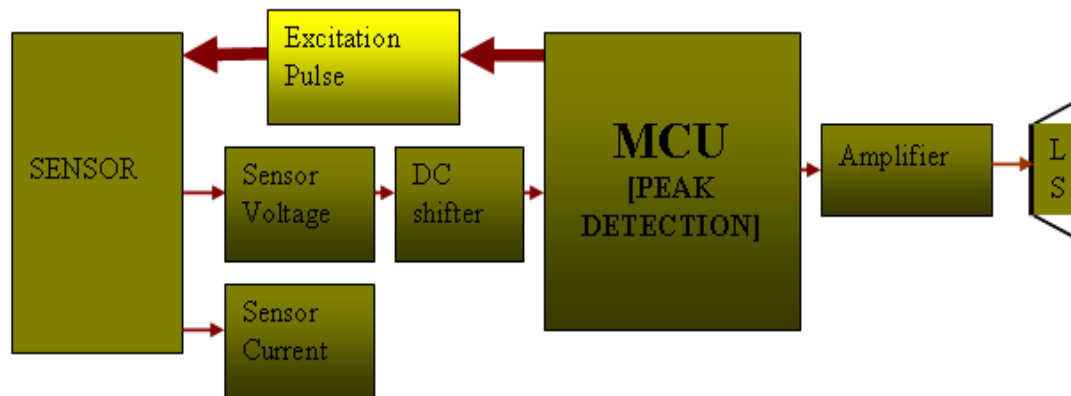
Fig 3.2   Block Diagram representation of the Portable Metal Detector

Fig 3.2 shows the detailed block diagram of the desired instrument. The instrument has mainly four blocks.

- Sensor

- DC shifter

- Microcontroller

- Loud speaker

The first two blocks are discussed in detail in Chapter3. The remaining blocks are described in Chapter 4. The proposed sensor is a differential type inductive proximity sensor as described above. It uses close-in excitation. When a metal target come closer to the sensor some eddy current is induced in the metal that changes the magnetic field associated with the receiving coil. This change in the magnetic field is sensed and a

differential voltage will be generated at the output of sensor. But for conductive targets, which are mostly paramagnetic, the differential output voltage is positive. And for inductive targets, the specific voltage is negative. So before giving this sensing probe voltage into the microcontroller, a dc voltage is added so as to make the final output voltage becomes positive. The system is designed based on Atmel ATXMEGA128A1 microcontroller which acts as a data acquisition processing system. The output voltage is connected to the analog input port of ADC and converted into digital form. The microcontroller first determines the maximum and minimum in the sample and generates a sound corresponding to the difference between the two values.

3.2 SENSOR

The proposed sensor has an air cored coil [7]. Normally PI detectors are using a single coil. The sensor diameter should follow the standard of keyhole surgical tool. Because of this constraint, it is very difficult to identify the target with a single coil. Therefore to increase the detection depth, differential sensing scheme along with a secondary conductor is used .The effectiveness of differential sensing scheme to achieve longer detection depths can be theoretically explained as below. Here a special former was designed as shown in Figure 3.3.
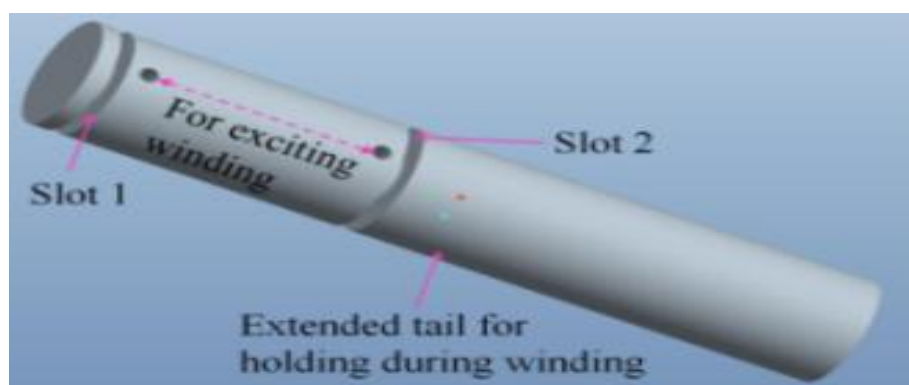
Fig 3.3 IPS Former Design [6]

There are two slots in the former. The slots accommodate the sensing and dummy coils and approximately 25 turns of 0.14mm thick conductor are kept in each slot. So by this arrangement the number of turns of the coil which is exposed to the eddy current flux from the target increases. Hence, the detection depth increases when compared to single coil IPS.
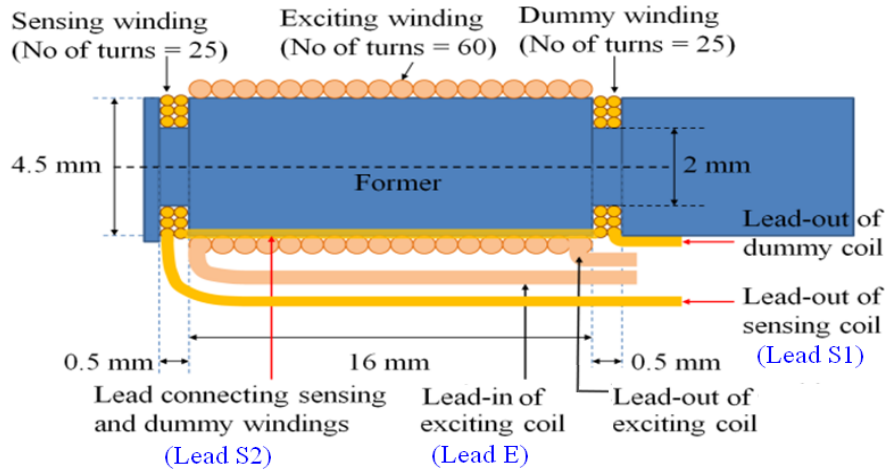
Fig3.4 Assembled View of IPS Sensor[6]

The equation 3.1 indicates the relationship between magnetic flux density (B) and diameter of a single coil. It is clear from the equation that the magnetic flux density (B) is inversely proportional to the diameter of the coil.

$$B = \frac{\mu I}{2\Delta t} \left[\frac{(z+n\Delta t)}{\sqrt{(r^2+(z+n\Delta t))}} - \frac{z}{\sqrt{(r^2+z^2)}} \right]$$

3.1

Here B is the magnetic field produced by a coil (or IPS) of radius r, n number of turns and length l at a distance z with a current I and μ being the permeability of the medium. Figure 3.2 represents the value of B for a distance of z=20mm.
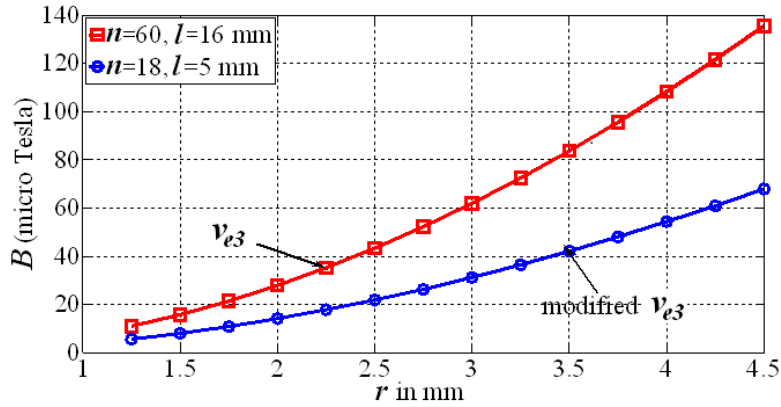
Fig 3.5 B at a depth of 20 mm for versus r for two different n and l [6]

From the graph in Fig 3.5 it is clearly understood that, the B value is small for smaller values of radius. Hence the detection depth will be small for IPS with small radius. If the system uses single conductor coil, then the detection depth is equal to their diameter. So differential sensing scheme is preferred over the single conductor method.

3.2.1 Features of IPS Sensor

Following are the main key features of the new IPS sensor.

1) Elimination of Parasitic Impedance

Here the former was specially designed as explained earlier. So by placing the sensing and dummy coil onto the same former, the parasitic impedances such as Z_p and Z_s are removed from the instrument. This arrangement gives the sensing coils, full exposure to the eddy current flux thereby increasing the detection depth.

2) Optimization of Number of Turns

Here the diameter of the exciting conductor was chosen as 0.28mm which could carry a current of 0.1A [6]. But here the excitation may last only for less than 1ms; the excitation current can be 3.5A RMS. But this is given, by ensuring the safety of the conductor. This high current helps to increase the eddy current flux from the target. The plot of B versus number of turns, n is given in Fig 3.6.
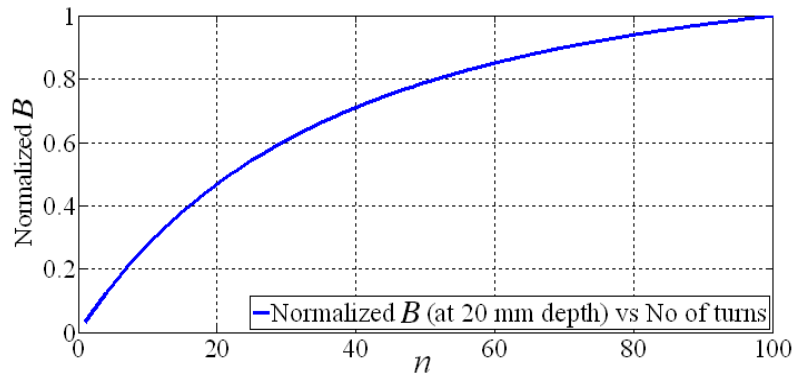
Fig 3.6 B versus n for IPS sensor [6]

From the figure, it is obvious that B increases with n and reaches saturation. But to maintain the supply current at 3.5A, we cannot increase the coil impedance. Considering these criteria optimally the number of turns for the sensing coil was chosen at 60.

3) Effect of Distance between Sensing and Dummy Coils

Since the dummy coil is kept nearer to the sensing coil, the magnetic field of dummy coil may get affected by the target. So the differential output taken in between sensing coil and dummy coil will get reduced. From calculation it is found that the effect of change in differential voltage for the IPS sensor is less. Here the distance between sensing and dummy coil is equal to the length of the exciting coil.

4) Effect of Offset Voltage (V_{os})

The sensing and dummy coils are hand-wound. If there is some constructional difference between the two coils, it will lead to an offset voltage V_{os}. This may lead to some difficulty in detecting the target. Another factor which will increase the V_{os} is the effect of parasitic impedance Z_e of the connecting lead between sensing and dummy coils and the inductance of the lead out of the sensing coil. In order to reduce the effect of offset voltage V_{os}, both sensing and dummy coils are wound planar in the new IPS. The width of the slots for both coils is set such that each new turn would fall exactly above the previous one without any nonalignment and hence both the coils are closely matched. The effect V_{os} can further be reduced by decreasing the length l of the exciting coil. But the problem is, this in turn reduces B at a distance. In order to retain the same B at a distance, the radius of the exciting coil has increased to 3.5 mm and n was reduced to 18. But shortening of length, gives only 60% of differential voltage V_d at the output. The features of the sensor are given in Table 1

Table 3.1 Features of the Sensor

Sensor Features	Values
Core	Air-cored
Thickness of exciting coil conductor (mm)	0.28
No of turns of exciting coil	18
Length of exciting coil conductor (mm)	560
Inductance of exciting coil (μH)	2.5
Resistance of exciting coil (Ω)	0.7
Thickness of secondary coil conductor (mm)	0.14
No of turns of secondary coils	16
Length of sensing/dummy coil conductor(mm)	230
Inductance of secondary coils (μH)	1.3
Resistance of secondary coils (Ω)	0.7

3.2.2 Close in Excitation

The circuit diagram for the excitation is given in Fig 3.7. The excitation [6] to the coil is given by discharging of a charged capacitor. It has three phases .1) charging phase 2) discharging phase 3) delay phase

a) Charging phase   b) Delay phase   c) Discharging phase
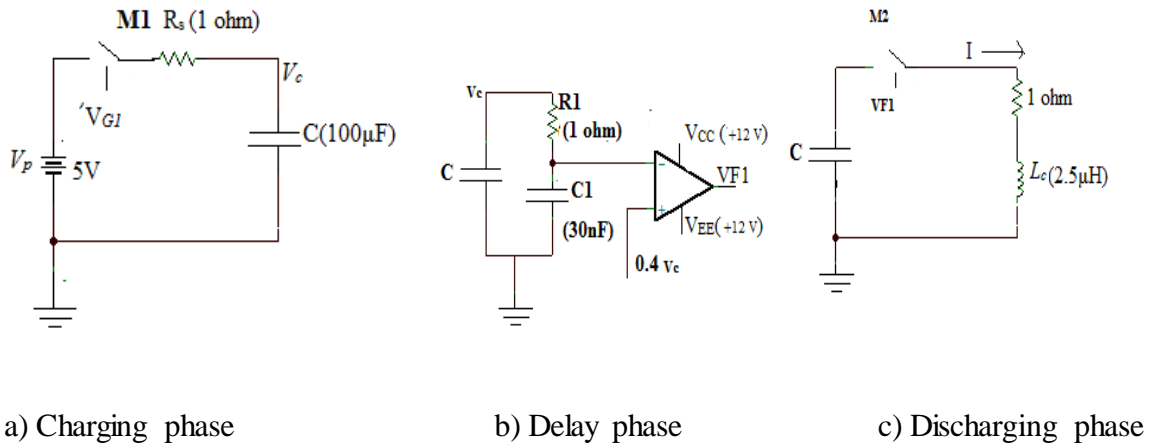
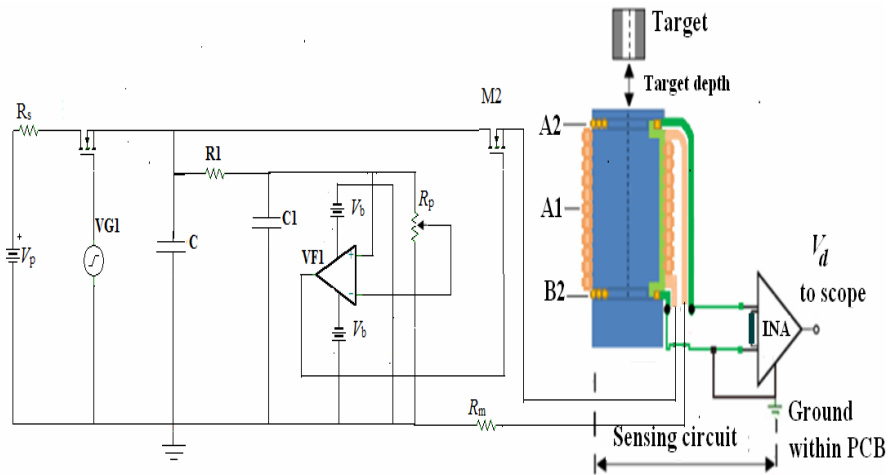Fig 3.7 Different phases of the Close-in excitation Circuitry [6]

Fig 3.8 Circuit Diagram of Close-in Excitation [6]

During charging phase the trigger which is of 1.5 ms pulse width is given to the gate (VG1)to the MOSFET (M1).The capacitor starts charging from a dc voltage and holds a voltage according to the following equation 2

$$V_c(\text{t})= V_p\left(1 - e^{-\frac{t}{R_sC}}\right)$$ 3.2

The values of R and C such that at the end of VG1 the capacitor should hold a value of 5V. During the delay phase the capacitor C will act as a battery to C1. Capacitor C1 starts charging from some 0.2 V_p. This voltage V_{c1} is compared against a reference voltage 0.4 V_c. In the discharging phase the gate pulse to the second MOSFET (M2) is given. When the voltage across the capacitor C1 exceeds the voltage across R_p, the output VF1 becomes high. This pulse switch on the MOSFET M2 and capacitor C discharges in to the exciting coil A1 (with inductance L_c) and the current I generate is measured across a current measuring resistance R_m as voltage V_p. The equation for I is given by 3.3

$$I(\text{t}) \;=\; \frac{Vc}{Rm\sqrt{\left(1+\frac{4Lc}{C.Rm^2}\right)}}\left[e^{-\left(\frac{Rm}{2Lc}-\sqrt{\left(\frac{Rm}{2Lc}\right)^2-\left(\frac{1}{Lc\,C}\right)}\right)t} \;-\; e^{-\left(\frac{Rm}{2Lc}+\sqrt{\left(\frac{Rm}{2Lc}\right)^2-\left(\frac{1}{Lc\,C}\right)}\right)t}\right]$$ 3.3

3.3 DC SHIFTER

Most analog to digital converters have a unipolar input that can be a problem when designing bipolar circuits. Here the ADC input voltage range from 0 to 2V. However the analog circuit (sensor) have voltage range from -1.5 V to +1.5 V . Bringing the ADC input below ground is not good, because the current from input will flow

through the chip substrate creating irreversible changes in the ADC and damage it. So, there comes the need of a dc shifter.
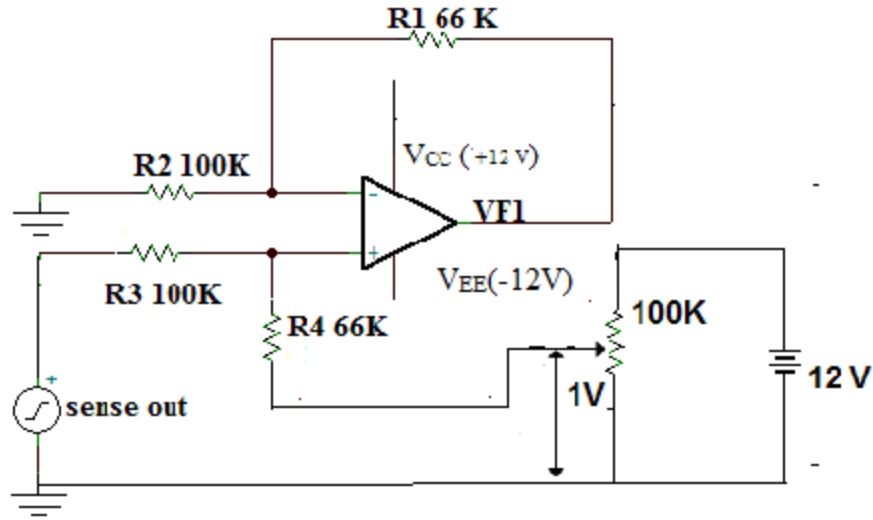
Fig 3.9 Circuit Diagram of DC Shifter

Fig 3.9 is the circuit diagram of the dc shifter. Gain without considering the offset is calculated using the following equation 3.4

$$A_{gain} = \frac{R4}{R2}\left[\frac{R2+R1}{R3+R4}\right] \qquad 3.4$$

So if choose R2=R3 and R1=R4

$A_{gain} = \dfrac{R4}{R2}$. Here we want to convert the 3 V peak to peak voltages into 0 to 2 V. So the gain factor is 0.667. If we choose the resistor R4=R1=66KΩ, then R3=R2=100KΩ.Gain with offset is calculated using the equation given 3.5

$$\text{So } A_{offset} = \frac{R3}{R2}\left[\frac{R2+R1}{R3+R4}\right] \qquad 3.5$$

19

So by default the offset gain is at one. So if we want to maintain the centre at 1V feed the reference voltage at 1 V.

CHAPTER 4

THE WORKING OF MICROCONTROLLER

The microcontroller ATXMEGA 128A1 is used to process the sensor output. The Atmel AVR XMEGA **[7]** is a family of low power, high performance, and peripheral rich 8/16 bit microcontrollers based on the AVR enhanced RISC architecture.

Fig 4.1 Showing Connections to the Evaluation Board ATXMEGA 128A1U

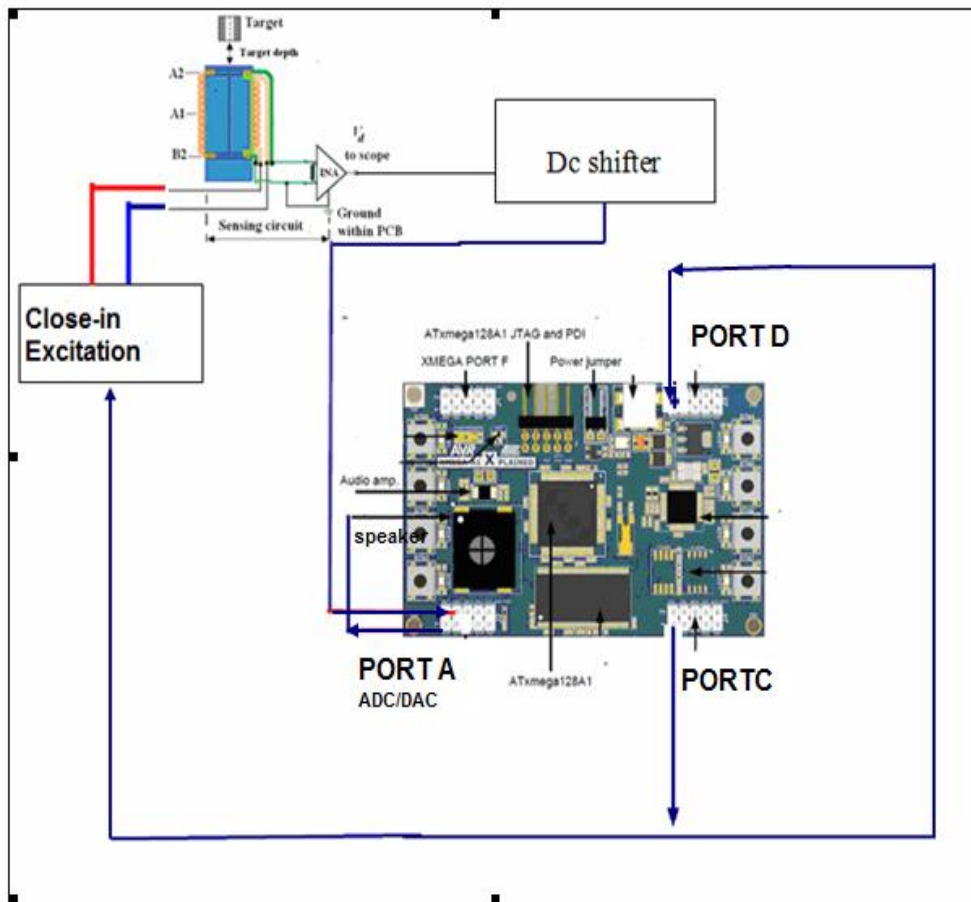The entire instrument is developed around the Atmel ATXMEGA-A1 Xplained evaluation kit [7] is a hardware platform to evaluate the Atmel ATXMEGA A1 microcontroller.

The kit offers the following features

- Atmel ATXMEGA 128A1 microcontroller

- External memory

  -8MB SDRAM

- Analog input (to ADC)

  -Temperature sensor

  -Light sensor

- Analog output (from DAC)

  -Mono Speaker via audio amplifier

- Digital I/O

  -Eight mechanical button switches

  -Eight LEDs

  -Eight spare analog pin

  -24 spare digital pins

4.1 ATXMEGA128 A1 microcontroller

The Atmel AVR XMEGA [8] a family of low power, high performance and peripheral rich 8/16 bit microcontroller based on the AVR enhanced RISC architecture. By executing instructions in a single clock cycle, the AVR XMEGA devices achieve CPU throughput approaching one million instructions per second allowing the system designer to optimize power consumption. The operating voltage for this microcontroller is 0-3.3V.The maximum frequency that can be obtained from the controller is 32MHz.

The following are the main features of the ATXMEGA microcontroller.

- 8/16 bit microcontroller

- Non-volatile program and data memory

    o 64K-128Kbytes of In –System self programmable flash

    o 4K-8K Bytes boot section

    o 3K Bytes EEPROM

    o 4KB-8KBytes boot section

- Peripheral features

    o Four channel DMA controller

    o Eight channel event system

    o Eight 16 bit tuner/counters

- Two sixteen channel, 12-bit 2msps Analog to Digital Converters.

- Two two channel,12-bit MSPS Digital to Analog Converters

- External interrupts on general purpose I/O pins

- Special microcontroller features

    o Power–on reset and programmable brown _out detection

    o Internal and external clock option with PLL and prescaler

    o Programmable multilevel interrupt controller.

- 78 programmable I/O pins.

- Operating voltage

    o 1.6-3.6V

- Operating frequency

    o 0-12MHz from 1.6V

    o 0-32MHz from 2.7 V

In these features some features which is used by this project needs some more explanation.

4.1.1 CPU

All Atmel AVR XMEGA devices use the 8/16 bit AVR CPU [8]. In order to maximize the performance and parallelism, the AVR CPU uses Harvard architecture. Instructions in the program memory are executed with single level pipelining. The 32×8 bit general purpose working registers all have single clock cycle access time allowing single cycle arithmetic logic unit operation between a register and immediate. The data memory space is divided into I/O register, SRAM and external RAM .In addition the EEPROM can also be mapped in the data memory .The Atmel supports inbuilt hardware multiplier which gives 16 bit result.

4.1.2 Memories

The Atmel AVR architecture has two main memory spaces the program memory and the data memory. All memory spaces are linear and require no memory bank switching, The Atmel AVR XMEGA device contain on chip, in system reprogrammable flash memory for program storage. All CPU instructions are 16 or 32 bits wide, and each flash location is 16 bits wide.

The flash memory is organized into two main sections, the application section and the boot loader section. The data memory contains I/O memory, internal SRAM, optionally memory mapped EEPROM, and external memory if available.

4.1.3 T/C -16 Bit Timer /Counter

Atmel XMEGA devices have a set of eight 16 bit Timer/Counter. A tuner/ counter consists of a base counter and a set of compare or capture (CC) channels. The base counter has direction control and period setting that can be used for timing. The CC channels can be used together with the base counter to do compare match control, pulse width wave modulation as well as various input capture operations. A timer can be clocked from the peripheral clock with optional prescaling. The event system can also be used for direction control and capture trigger. There are two differences between timer/ counter type 0 and type 1. Timer/Counter0 has   four Compare /capture channels, and timer/counter1 has two CC channels.

4.1.4 System Clock and Clock Options

An Atmel AVR XMEGA device incorporates both internal oscillator and external crystal oscillator. It have 32MHz run-time calibrated RC oscillator 2 MHz run-time calibrated RC oscillator, 32.768 KHz calibrated RC oscillator, 32KHz Ultra Low Power(ULP) oscillator with 1KHZ output as internal oscillators. Fig 4.2 shows the different clock system and clock sources of the ATXMEGA128 A1U. The external clock options are 0.4-16MHz Crystal Oscillator, 32 KHz Crystal Oscillator and External clock. The built-in phase locked loop (PLL) can be used to generate a high frequency system clock. The PLL has a user selectable multiplication factor from 1 to 31. In combination with the prescalers, a wide range of output frequencies can be derived.
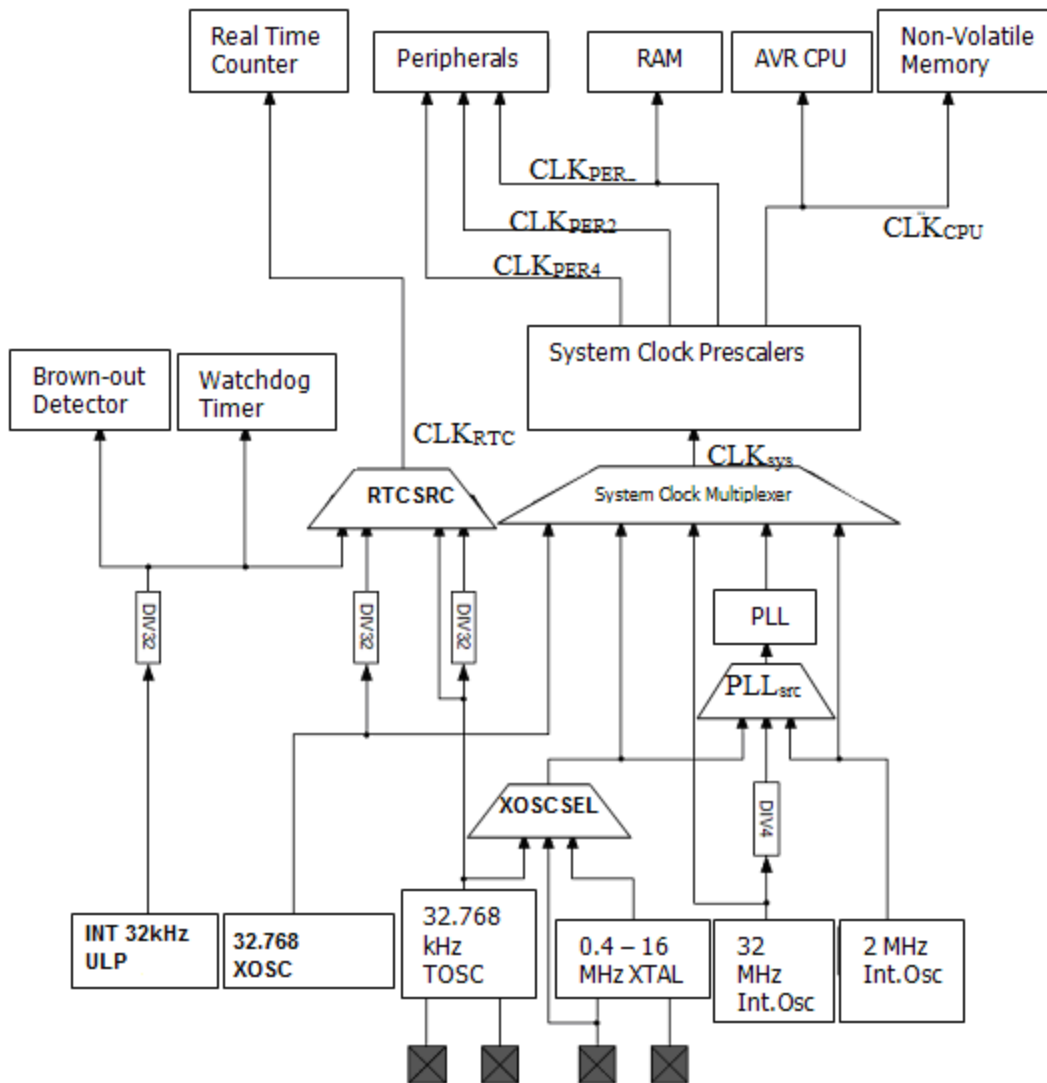
Fig 4 .2 Overview Of Clock System ,Clock Sources and Clock Distribution[8]

4.1.5 I/O Ports

XMEGA microcontrollers have flexible general purpose I/O ports. One port consists of up to eight port pins: pin 0 to 7. Each port pin can be configured as input or output with configurable driver and pull setting. They also implement synchronous and asynchronous input sensing with interrupts and events for selectable pin change conditions. Each port has one data direction (DIR) register and one data output value (OUT) register that are used for port pin control. The data input value (IN) register is used for reading the port

pins. In addition, each pin has a pin configuration (PINnCTRL) register for additional pin configuration. Port pins can generate an event when there is a change on the pin.
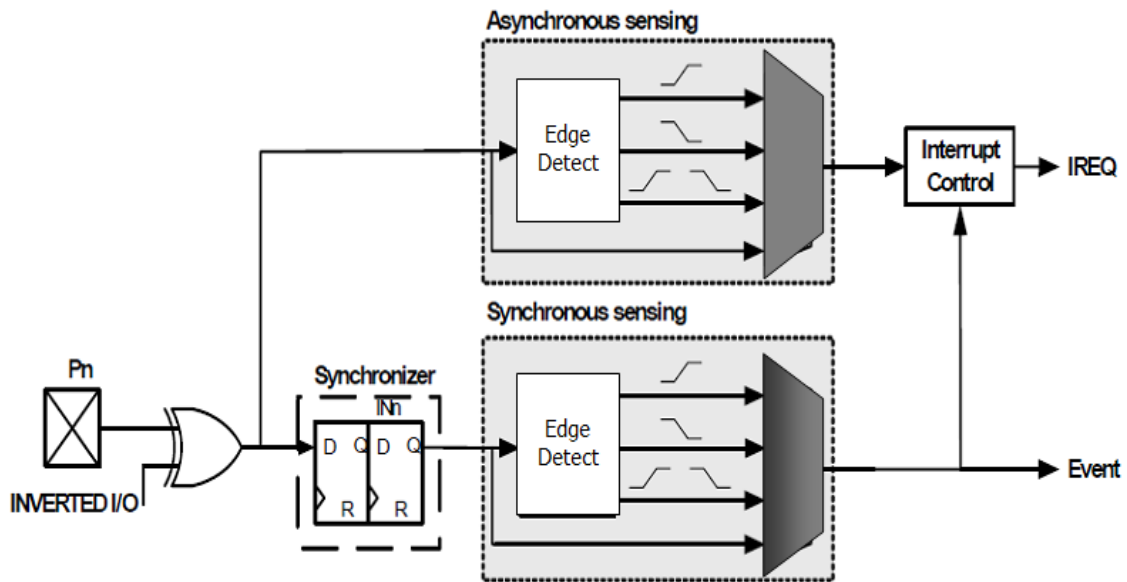

Fig 4.3 Input Sensing System Overview [8]

4.1.6 ADC-12 bit Analog to Digital Converter

The ADC **[9]** offers a high-performance ADC capable of conversion rates of up to 2Msps with a resolution of 12 bits. Xmega uses a pipelined ADC. The ADC can provide both signed and unsigned results. ADC measurements can be either started by application software or an incoming event from another peripheral in the device. It has 4 result registers with individual input channel control for each ADC.
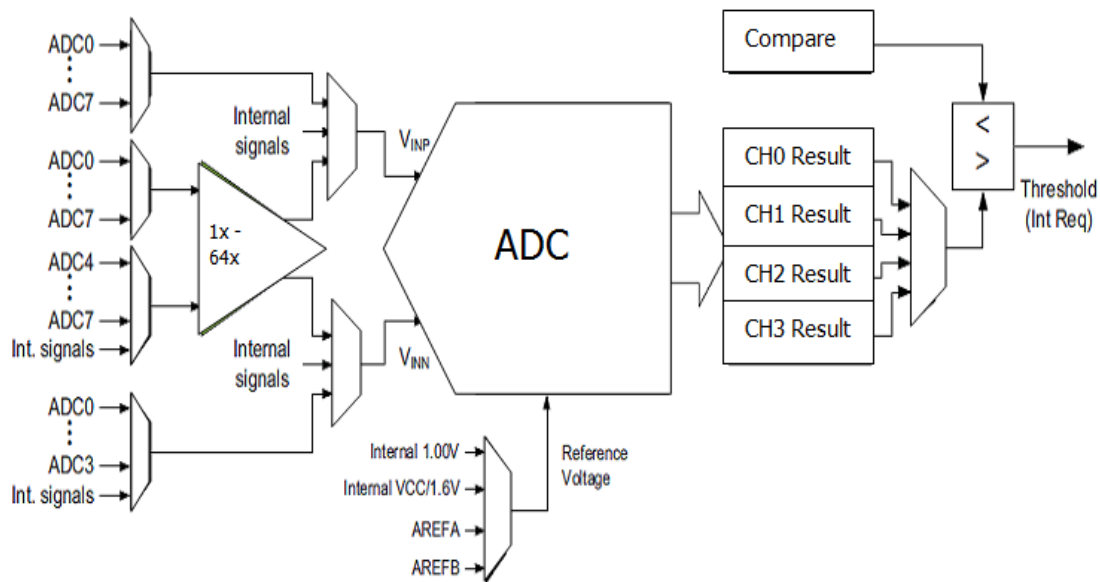
Fig 4.4 Overview of ADC [8]

Each ADC has four MUX selection registers with a corresponding result register. This means that four channels can be sampled within 1.5µs. The result is 12bit. So the left, right adjustment is also possible. The Atmel ADCs offer four modes

- Internal : Input sources are connected to internal analog signals (temperature, band gap etc)

- Single-ended: The negative input is connected to ground. The input source is connected to positive input.

- Differential without gain: The input signal is connected between positive and negative inputs.

- Differential with gain: A selectable gain modifies the input signal level before ADC conversion.

The ADC has two conversion modes

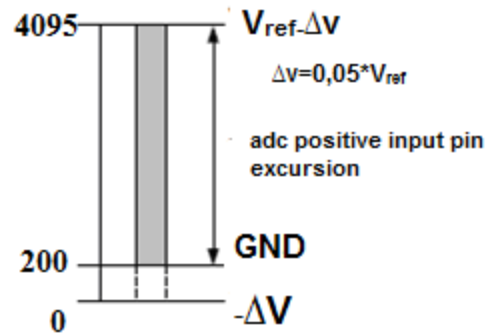1) Unsigned Single-ended mode and 2) Signed ended Mode

Fig 4.5 Unsigned single ended mode range

In unsigned mode, the conversion range is from ground to the reference voltage. The approximate value corresponding to ground is around 200. Fig 4.5 shows the unsigned mode range for the ADC. This mode offers full resolution (12 bits) and zero crossing detection. In signed mode the conversion range is from V_{ref} to $-V_{ref}$.

2) Signed Differential Input

The resolution is 11bit .When the gain stage is used, the input signal is amplified before it reaches the ADC.
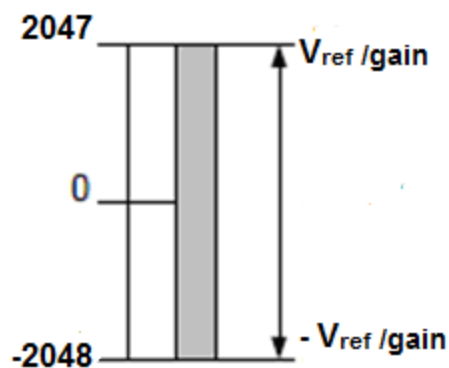

Fig 4.6 Signed Mode Range

There are mainly four types of voltage references. They are

- INT1V   -Internal 1V (Bandgap)

- INTVCC   –Internal V_{cc}/1.6

- AREFA   -External reference on AREF pin on PORTA

- INTVCC/2   -Internal V_{cc}/2

4.1.7 DAC-12bit Digital to Analog Converter

The XMEGA A1 devices feature two 12-bit, 1MSPS DACS [8] with built_ in offset and gain calibration. The DAC may use an internal 1.0 voltage as the upper limit for conversion, but it is also possible to use the supply voltage or any applied voltage in between. The external reference input is shared with the ADC reference input.
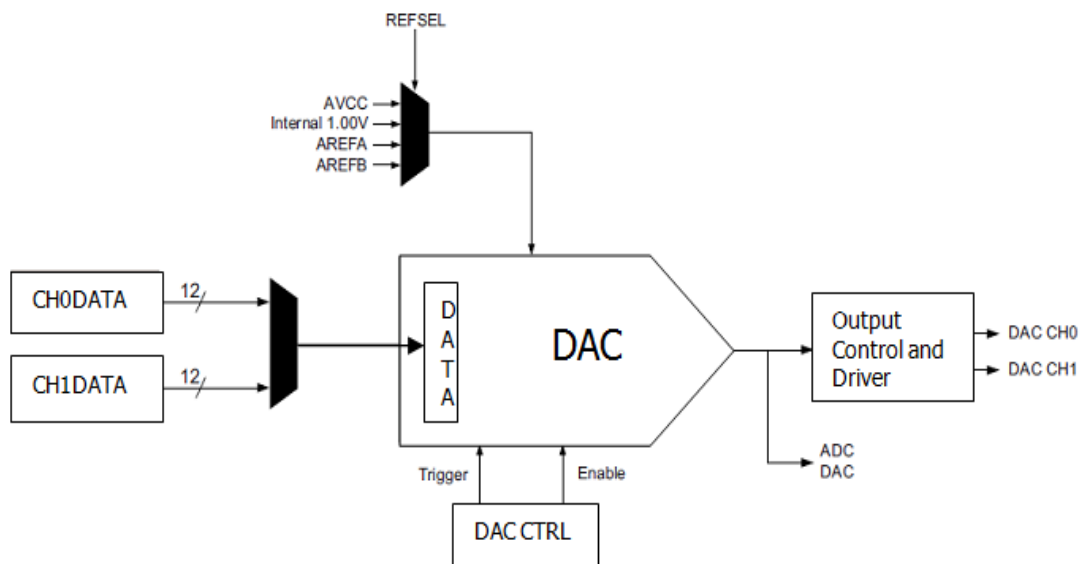

Fig 4.7 Overview of DAC[8]

Fig 4.7 represents the structure of DAC .The DAC can also be configured to do conversion triggered by the Event System to have regular timing, independent of the

30

application software. DMA may be used for transferring data from memory locations data registers.

4.2 SOFTWARE DEVELOPMENT

The program for microcontroller has been written after the testing of sensor and other parts of the circuit. The following software are used for writing and feeding programs in ATXMEGA128 microcontroller.

1. AVR STUDIO5: AVR studio5 is the development platform. AVR studio is required to write the C-code and generate HEX code.

2. Win AVR is used to compile the program.

Flowchart for the entire process is shown in Fig 4.11. The ADC's maximum operating frequency is determined from the CPU frequency and the maximum frequency for the ADC is quarter of the CPU frequency. For obtaining a 2MSPS sampling rate from ADC, the CPU frequency should be greater than 8MHz. In order to avoid the chance of missing samples in between the CPU executions, the controller frequency is chosen at maximum frequency of 30MHz. The entire process will start by generating a clock of 30MHz from the controller. The programming flow is explained as four different sections below.

4.2.1 Excitation Clock Generation

For the excitation of sensor, a trigger pulse should be given to gate of MOSFET (M1). This pulse should be of 2.5ms pulse width. From the above discussions it can be noted that the pulse repetition frequency is 1s. The normal operating frequency for ATXMEGA devices are 2MHz. But to obtain a CPU frequency of 30 MHz (almost maximum frequency) and to derive a sampling rate of 1MSPS for the ADC, the PLL is

selected as the system clock and using software the PLL can be configured. It is not possible to select a non stable or disabled oscillator as the clock source. PLL has a status flag that can be read from software to check whether the oscillator is ready or not. So by setting a multiplication factor of 15 for PLL, a clock of 30MHz (2MHz $\times$ 15) can be derived. The controller has two prescalers. By setting prescaler A and B with a factor of 1, the CPU frequency remains at 30MHz. After setting of the system clock, the excitation pulse to the sensor is produced. The inbuilt timers of the microcontroller have been used for the generation of pulse. For the generation excitation pulse, one of the TIMER0's is used. This is followed by delay routine. The flow of the particular process is shown in Fig 4.9
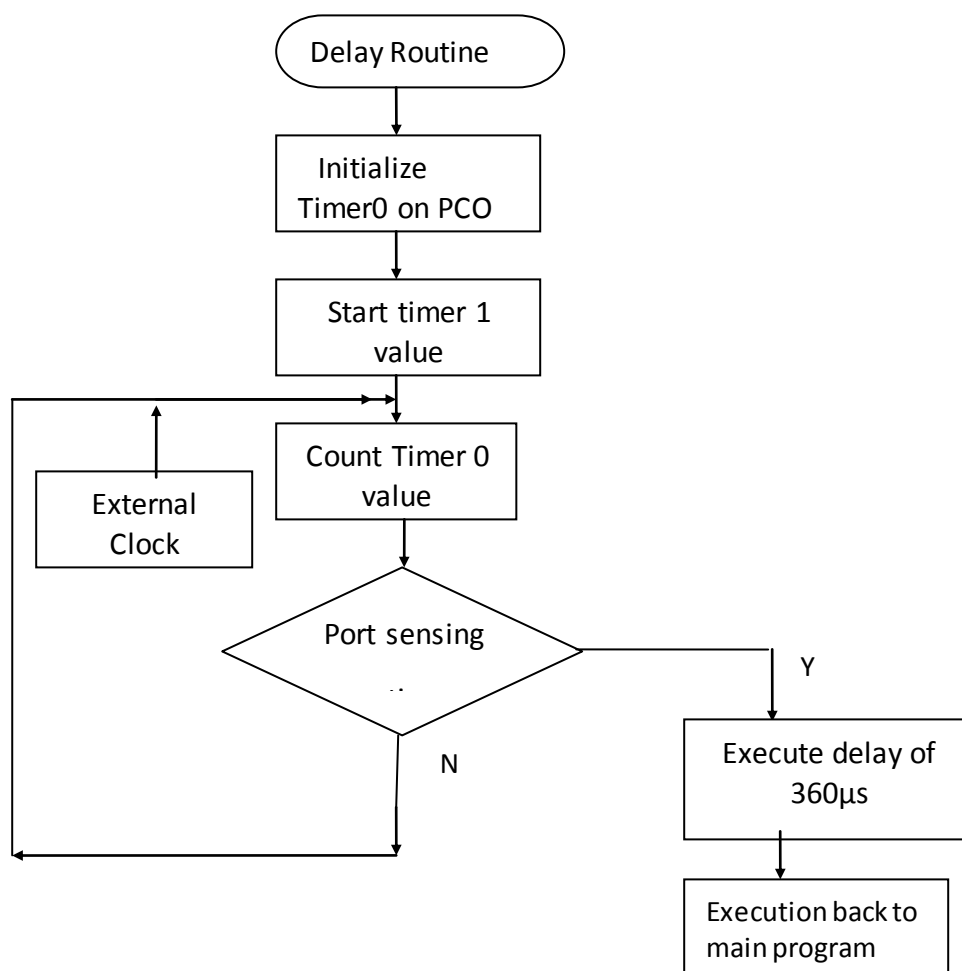

Fig 4.8 Flow chart showing the Timer working

The algorithm is so designed that TIMER 0 on PORT C (PIN PC0) is used as a timer. The pin PD0 on PORT D is driven by an edge sensing interrupt. The negative edge on the PORT C (PC0) is sensed by an interrupt as said earlier. This interrupt initiates a delay routine of 300μs on PORT D(PD0). The purpose of this interrupt sensing method is to limit the number of samples from the sensor output. From the sensor output, it is obvious that, the required data will start to appear in almost 300μs after the occurrence of negative edge of pulse on PC0. So the reading from the sensor will start only after 300μs of the negative pulse of the TIMER0 on PC0. This particular value (300 μs) is fixed by observing the sensor output. Here the timers have PER register and CMPx register. The period (T) is controlled by the PER register while the CMPx registers control the duty cycle of the waveform generator output. These register values are calculated using the following equation 4.1.

$$f = \frac{f_{PER}}{N(PER+1)} \hspace{4cm} 4.1$$

Where f_{PER} represents the peripheral clock frequency, N represents the prescaler and PER represents the frequency of peripheral.

The external pulse has been counted by TIMER0 on PC0 for 1 second. Now the samples are acquired by the ADC. For storing the analog input into the ATXMEGA 128 A1U, the microcontroller should be initialized and configured as per requirement. TABLE 4.1 represents he initialization parameters of ADC

Table 4.1 represents the parameter setting of ADC

PARAMETERS OF ADC	Values
Sampling Rate	2MHz
Conversion Mode	Single ended
Gain	Unity
Channel Selection	Channel 0
Pin	PIN0 of ADC
Reference	Internal Vcc/1.6

The algorithm for storing analog voltage values with the use of ADC is shown in Fig 4.10. The conversion will not be completed until the interrupt flag in the INTFLAGS has become high. After successful conversion the digital outputs are stored in respective registers that is RESH and RESL value.
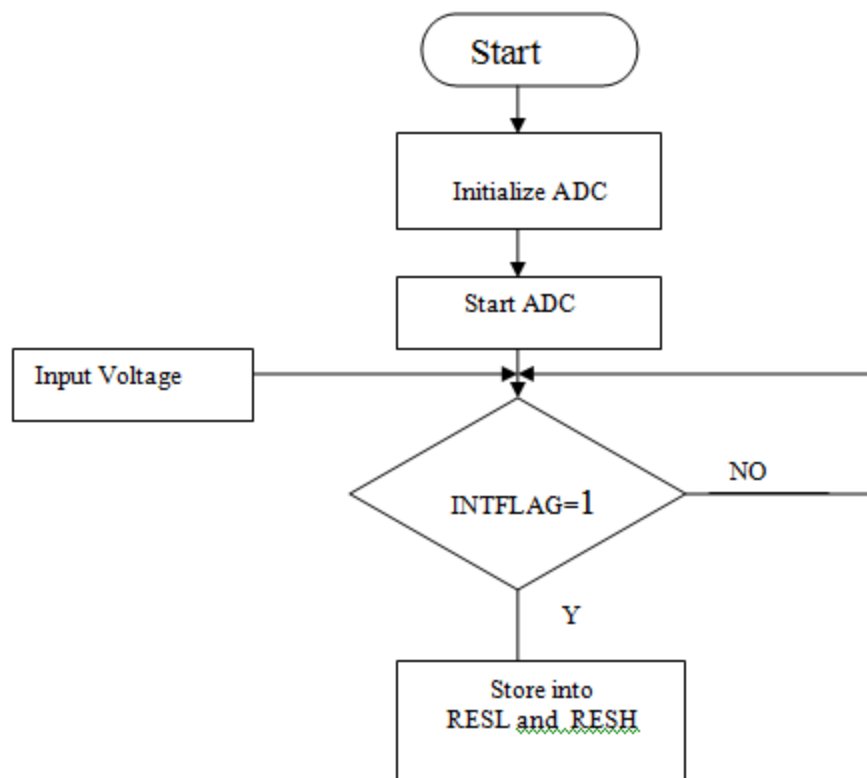

Fig 4.9 Showing working of an ADC

The detailed algorithm which is used for generating the sound corresponding to the processed sample value is shown in Fig 4.11. The first step of the program will be the

initialization for the generation of exciting pulse. The algorithm used for converting analog voltage into digital form and the procedure for storing data is given in the flowchart Fig 4.10. The first step is used for accruing offset voltage. The first data sample that is acquired will be stored as variable offset. This indicates the presence of offset voltage V_{os}. This calibration phase repeats for some 5 cycles. And its average value is found and stored as a final value in the variable offset. After the calibration phase, the original data samples which correspond to the target is acquired, then find out the largest and smallest values of the data and offset. Now calculate the difference between largest and smallest of target data (V_{tarr}) and offset (V_{off}). Then subtract V_{off} from V_{tarr}. The corresponding value is used to produce the sound. At every triggering pulse the above process is repeated except the calibration phase to identify the target.

For generating sound the inbuilt speaker of this evaluation board ATXMEGA 128A1 XPLAIN is used. Here the ATXMEGA has two DACs, DAC A and DAC B. The DAC B is internally connected to the audio amplifier. The audio amplifier should be enabled first, and the DAC should be initialized . The difference between V_{tarr} and V_{off} is loaded in DAC register and this value is used to modulate a triangular wave and this triangular wave controls the in built loudspeaker.
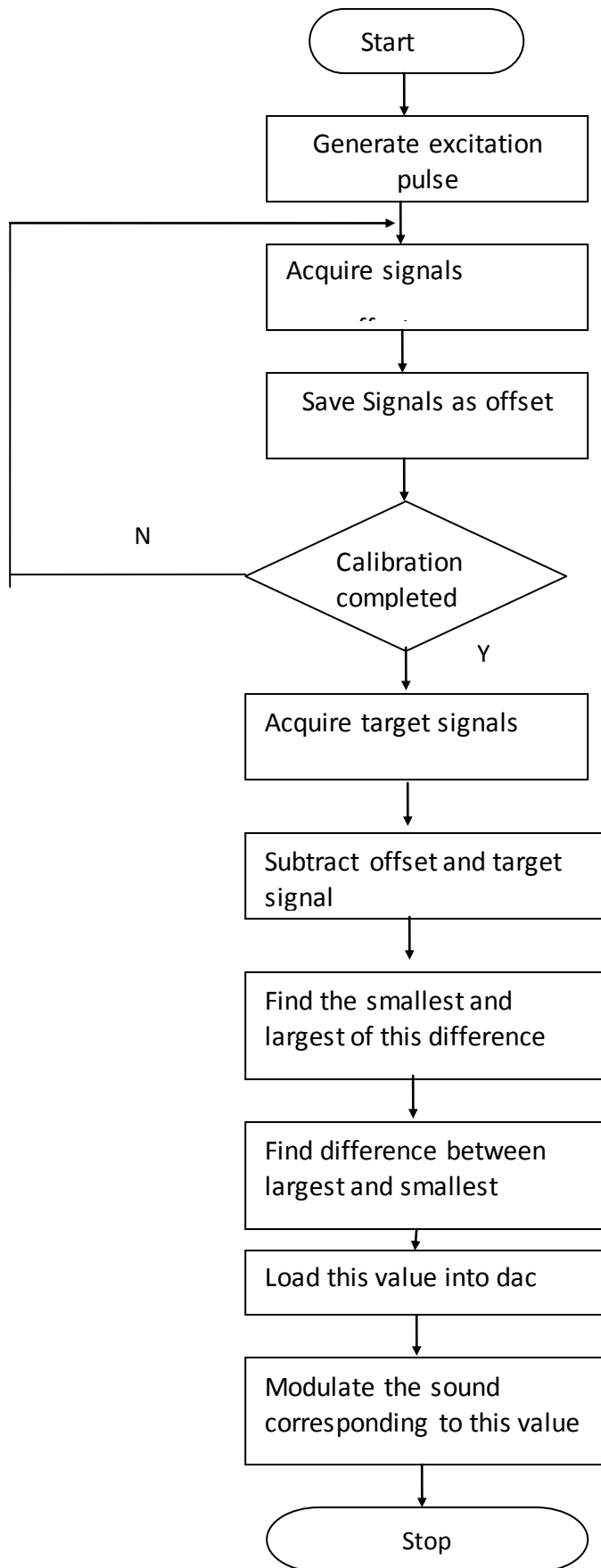
Fig 4.10 Represents the Entire working Flow of the Circuit

CHAPTER 5

TEST AND RESULTS

A microcontroller based miniature IPS sensor is developed. To determine whether the functionality described in Chapter3 and Chapter4 is implemented correctly or not, several incremental tests are performed. Not all tests produced interesting data, for example, initial test of the microcontroller for finding the peak of a triangle wave had given a wrong data. In this discussion the tests used to verify correct operation of the entire system is included. Here the sampling rate requires to process the sensor output is 1MSPS. This requirement ends in choosing the microcontroller ATXMEGA 128A1. The hardware for the entire circuit is designed by using the evaluation board ATXMEGA 128A1 XPLAIN from AVR. The evaluation board is shown in figure 5.1
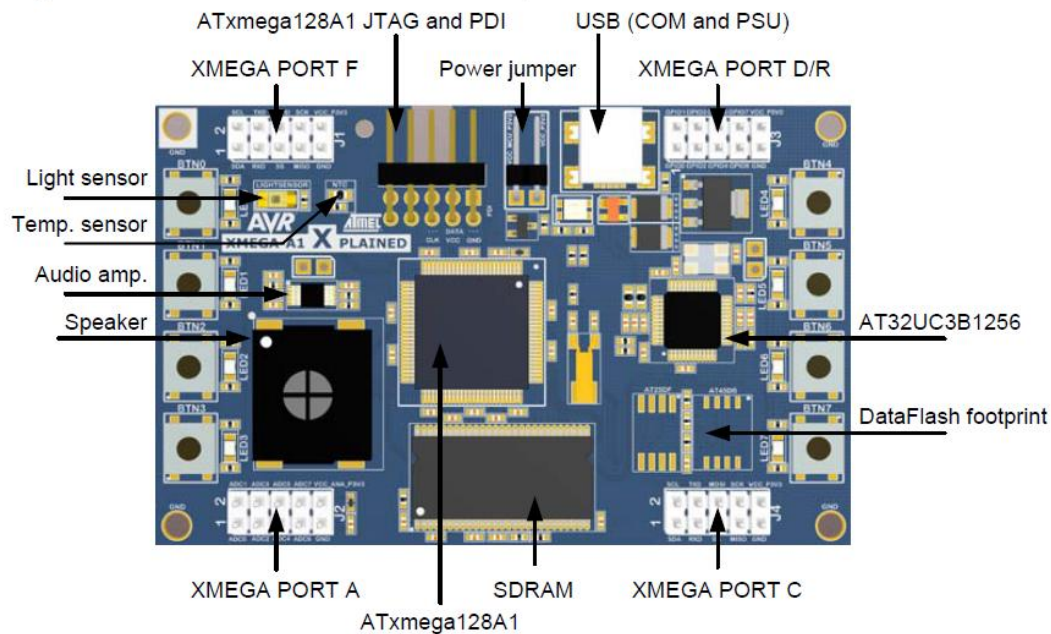

Figure 5.1 Evaluation Board of ATXMEGA 128A1U[8]

These evaluation boards provided all supporting circuits to the chip including power, oscillator connections, headers to make connections to the pins on the microcontroller etc. The attractive feature of this evaluation board is the inbuilt speaker which is used for generating sound in this project. The red colored circle represents the microcontroller, which operates using 3.3V supply. An experimental setup given in Fig 5.2 shows the connections between the sensor and the board.
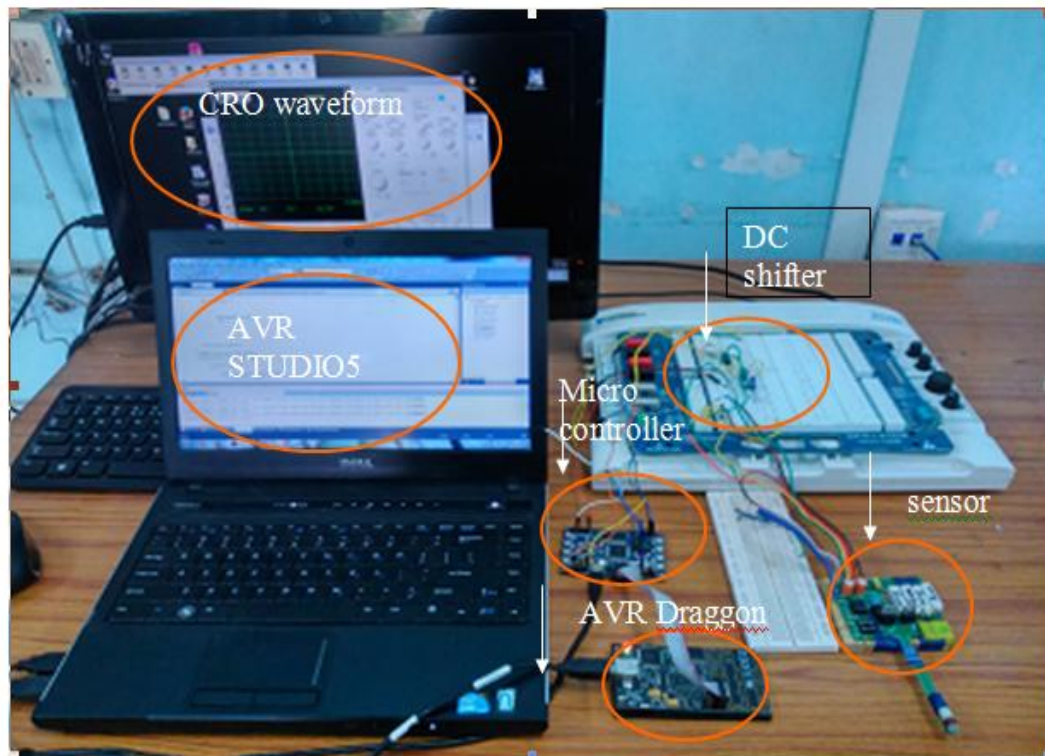

Fig 5.2 Experimental Setup for the IPS Sensor

The sensor is connected on board as depicted in the Fig 5.2. The trigger is given from ATXMEGA 128A1 through PORT C. A close-in excitation circuitry will excite the sensing coils as described above. The waveforms at different parts of the circuits are represented below.

5.1 TRIGGER PULSE

The sensor is initiated by giving trigger pulse from microcontroller. As discussed earlier, with the help of timers, the microcontroller produces the required pulse of width 2.5ms. The generation of this pulse is repeating in every 1s. Fig 5.3 shows the 2.5ms pulse and Fig 5.4 shows the repetition frequency for the pulse as 1s. The Timer 0 on PORT C is used for generating excitation pulse to the close-in excitation.
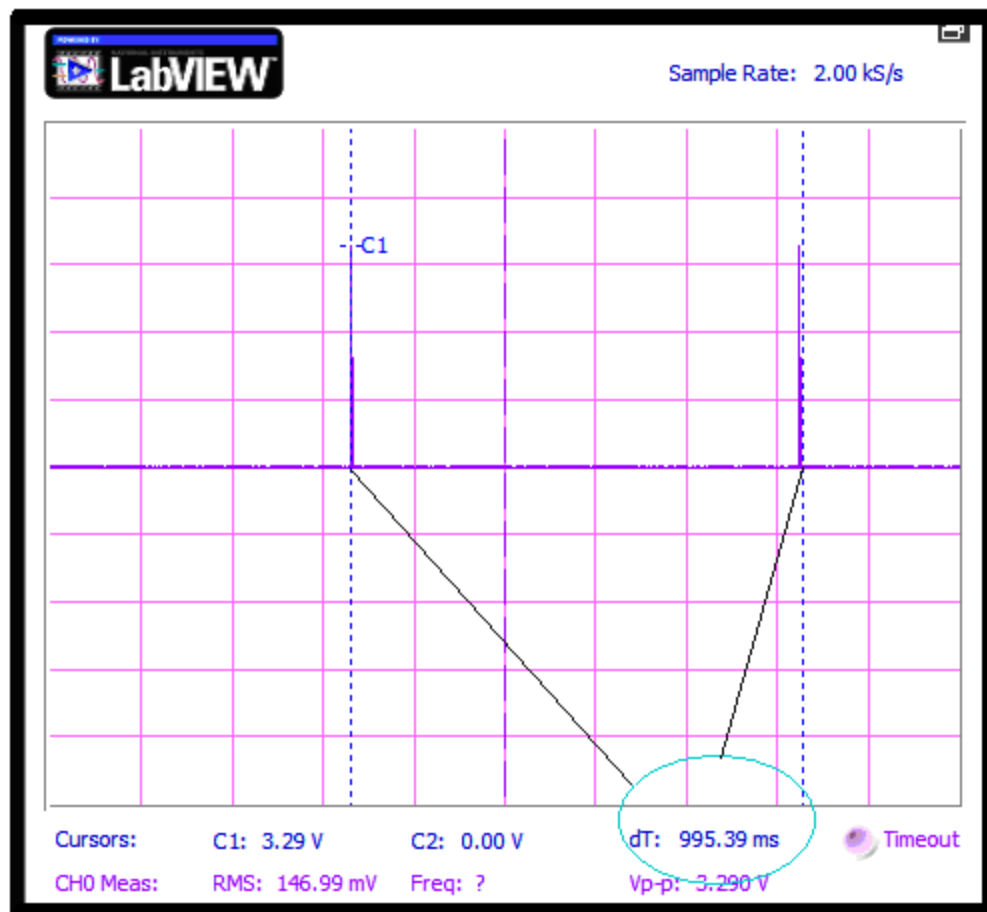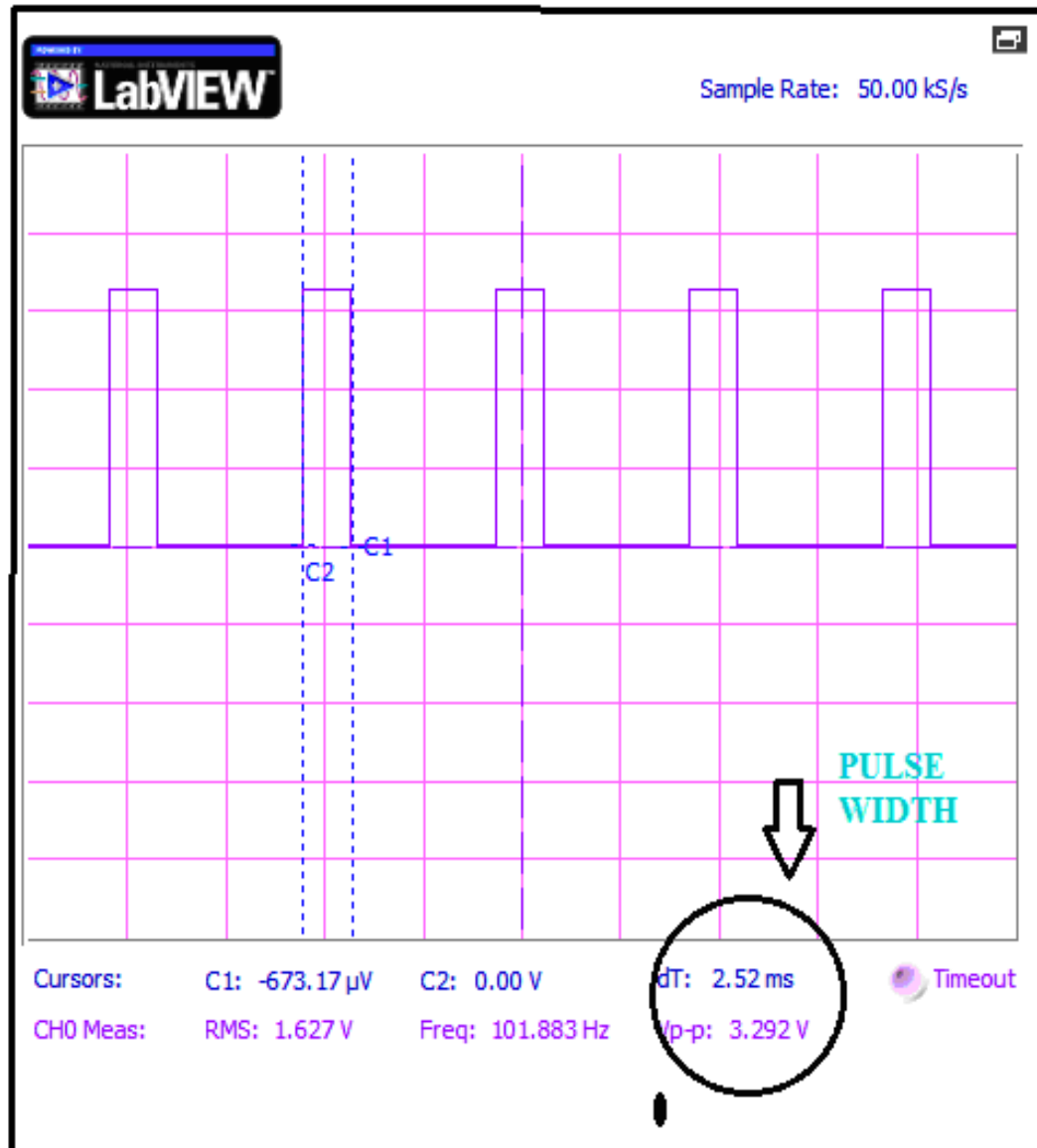

Fig. 5.3 Trigger Pulse showing the Pulse frequency

Fig 5.4 Trigger Pulse showing the pulse Width

5.2 SENSOR

To understand the performance of this instrument system, the developed sensor has been connected at the position. The Fig 5.5 given below shows the sensor
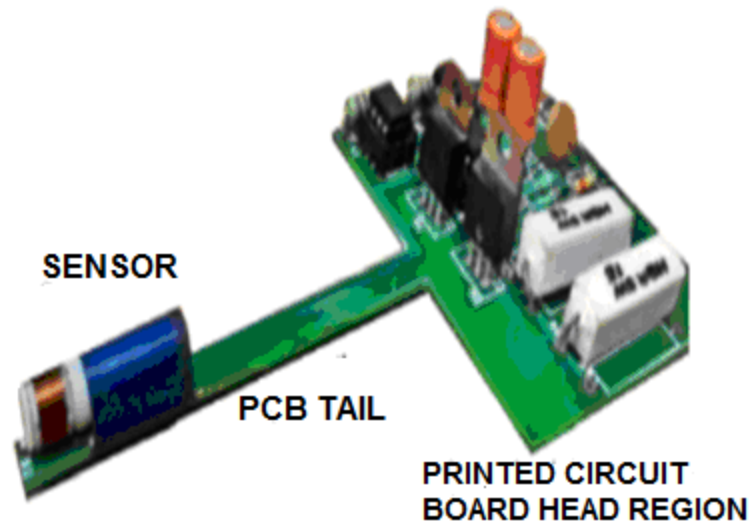
Fig 5.5 New IPS sensor [6]

5.2.1 Current Pulse

The excitation current from the sensing probe is given in Fig 5.6. A short term excitation current is obtained from the close excitation circuit.
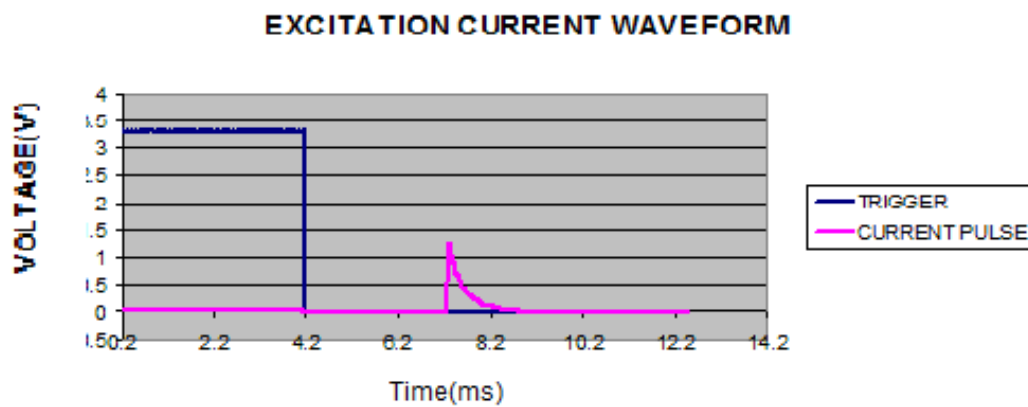

Fig 5.6 Trigger pulse and Excitation Current from Sensor

5.1.2 Sensor output without target
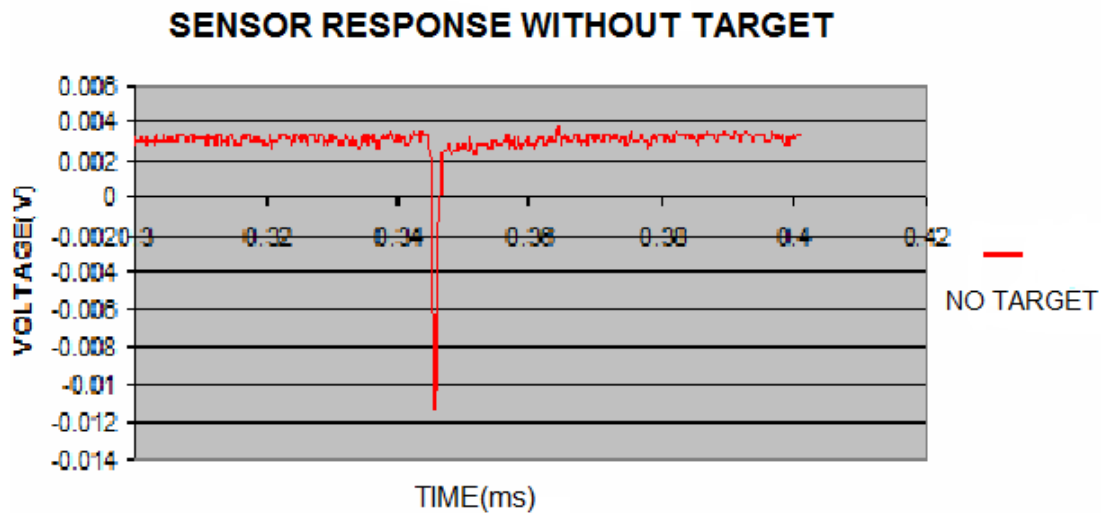
SENSOR RESPONSE WITHOUT TARGET

Fig. 5.7 Sensor output without target

The effect of the V_{os} is indicated in Fig 5.7. This output is of -12Mv, which is an insignificant voltage. This accounts for the effect of geometrical mismatch and parasitic inductance.

5.2.3 Response for Steel Target

The response for steel with nearest target position of 1mm is shown in Fig 5.8. Steel is a magnetic material. As the target comes nearer to the sensor the magnetic flux density will get increase. The red color indicates the sensor output and the yellow line indicates the trigger pulse that was generated from the microcontroller. The response for different target positions with same steel material is represented in Fig 5.9. From the

figure it is clear that the detection depths start from 9mm. A voltage of 900 mV is obtained as output for a distance of 1mm.
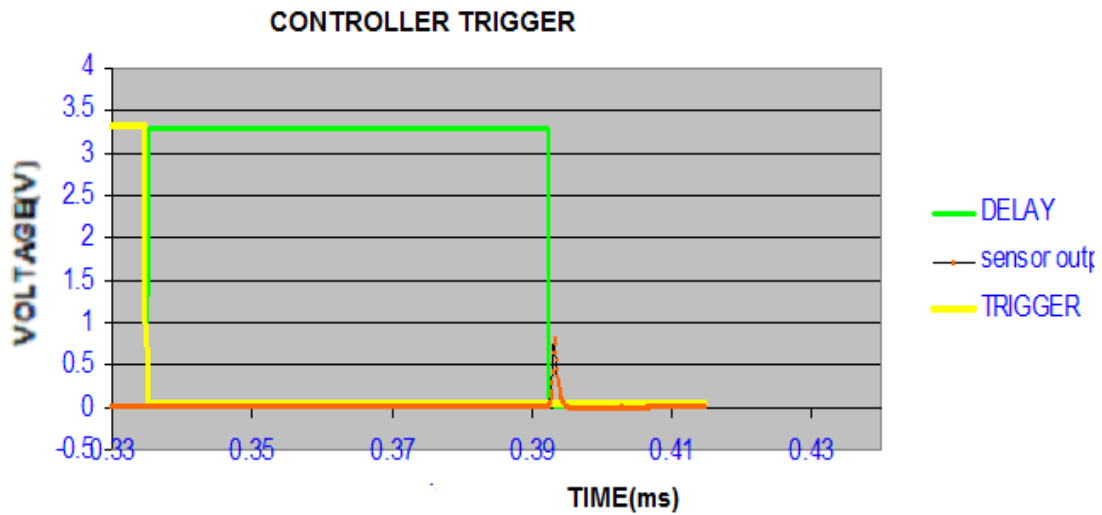

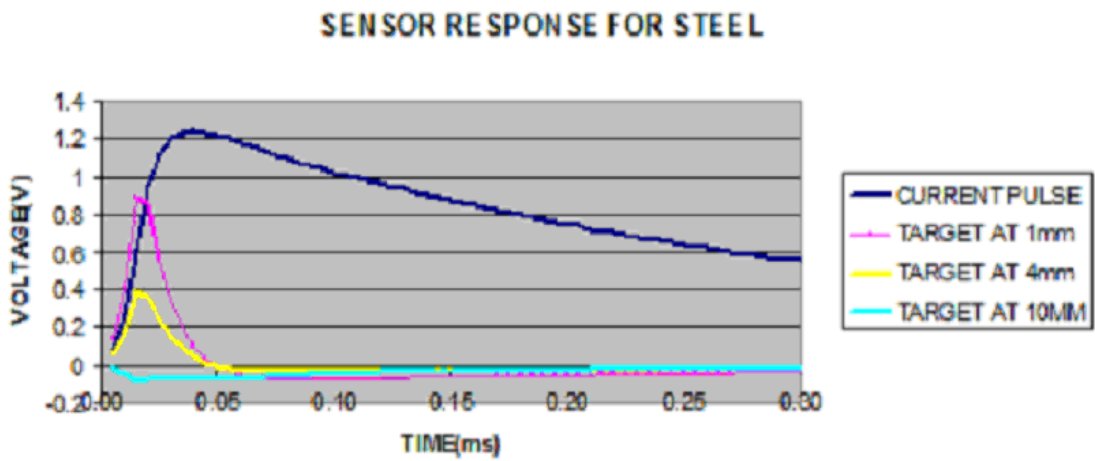Fig 5.8 Trigger pulse, Delay pulse, and sensor output to steel

Fig 5.9 Sensor response to steel for different distances

5.2.5 Copper response

The responses for copper with nearest target position of 1mm are shown in Fig 5.10. Copper is a nonmagnetic type material, as the target comes nearer to the sensor the magnetic flux density gets reduced. The response for different target positions with same copper material is represented in Fig 5.11. From the figure it is obvious that the detection depth starts from 8mm. A voltage of 600 mV is getting for distance of 1mm as output.
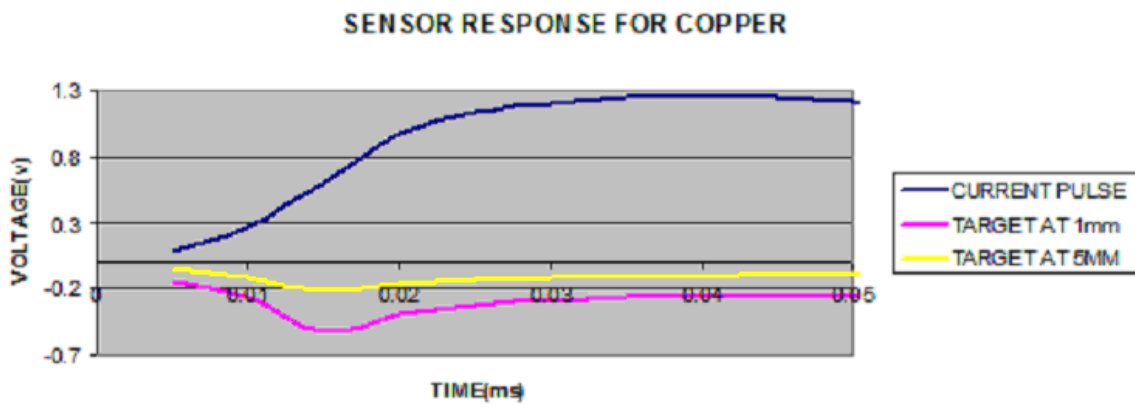

Fig 5.10 Sensor Response to Copper Target

5.3 Dc Shifter

In order to check whether the dc shifter is working fine or not, the sensor output is connected to the input of dc shifter and the output for a steel target with 3 mm outer dimension is shown in Fig 5.11. The red colored graph indicates dc shifted waveform. As indicated in the figure, after a delay time of 500 μs, the output is showing some progressive excursions. The response of the dc shifter for copper and steel is indicated in Fig 5.12 and 5.13.
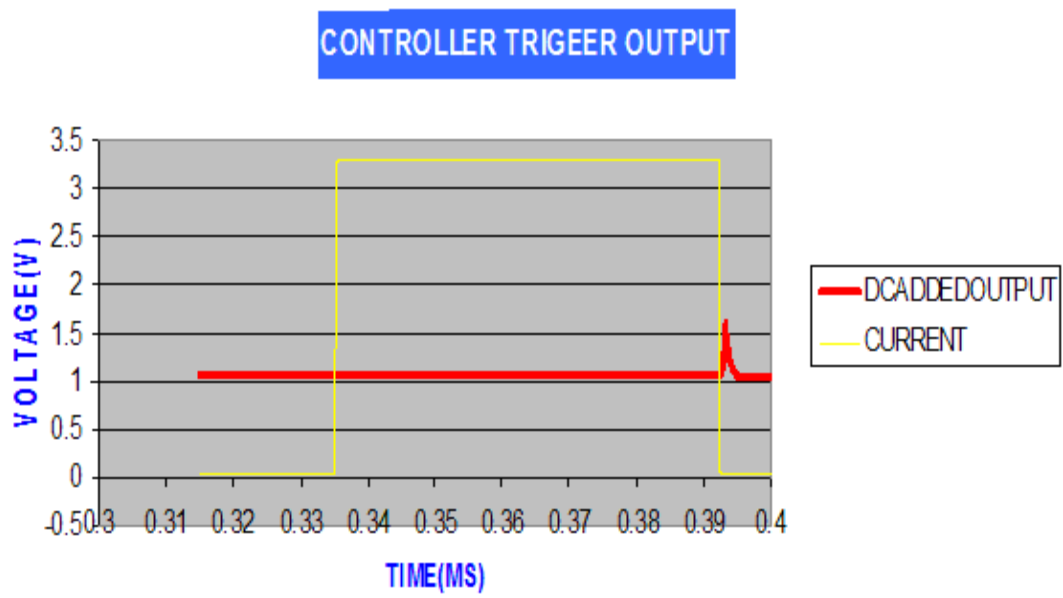
Fig 5.11 Dc shifted sensor output with delay pulse to steel
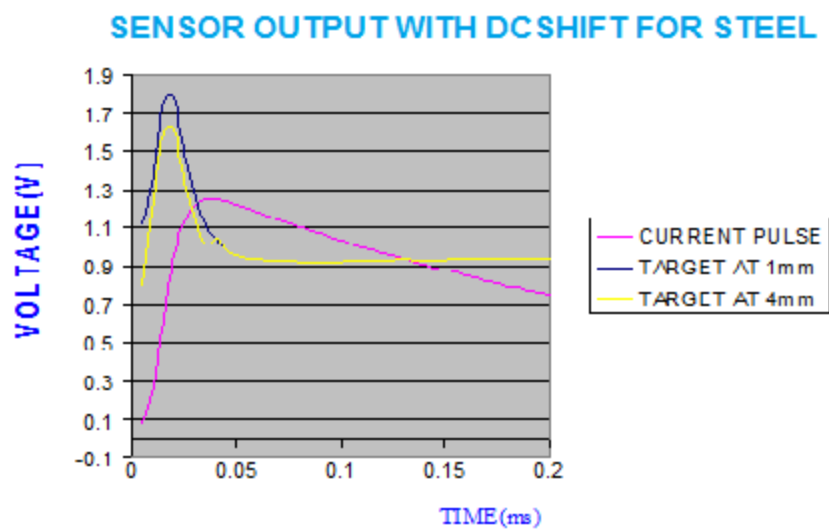

Fig 5.12 Dc Shifter sensor output for different distances to steel

It is clearly observed from the figure, that the sensor output is de-amplified and added with a dc voltage of 1 V. The response of dc shifter with different target distances is indicated in given Fig 5.14.
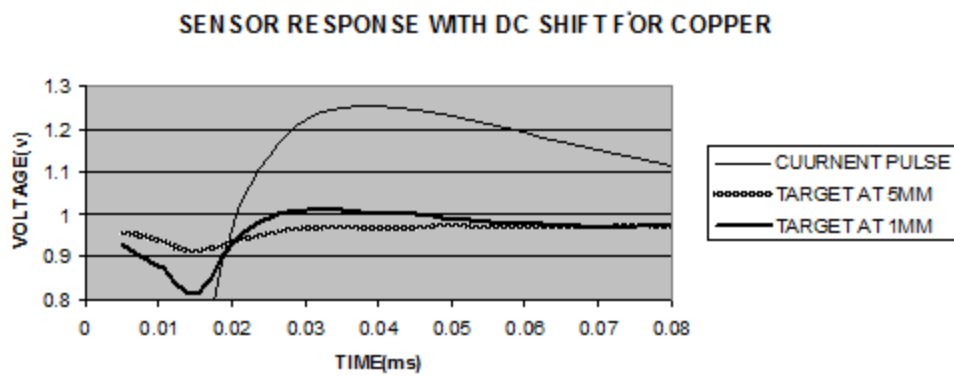

Fig 5.13 DC Shifter sensor output for different distances to copper
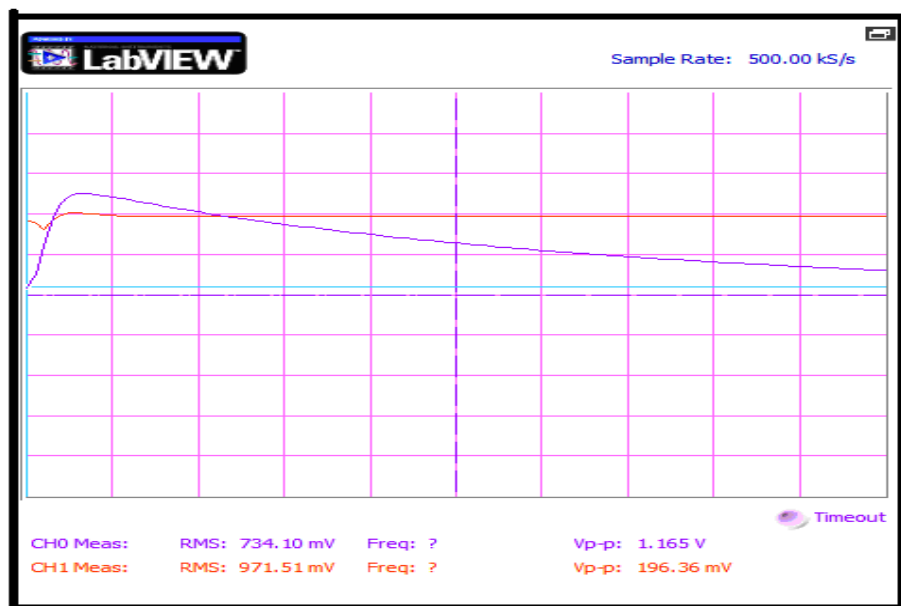

Fig 5.14 Oscilloscope waveform showing current pulse and dc shifted sensor output for steel

5.4 DAC Output

The sensor output is processed by the microcontroller as described in chapter 4. The peak value which is found by the microcontroller is loaded into DAC that will generate a voltage corresponding to the peak value. The response for the metal detector to different objects will almost gives the same result. The table given below shows the DAC output for different objects and the objects which is used for checking the response is shown in fig 5.15

Table 5.1show the DAC output for Different type of Material

SLNO	MATERIALS	DAC OUTPUT
1	Steel Nut	2.6 V
2	Copper Foil	2.5 V
3	Steel Screw	2.7 V
4	Gold	2.3 V

Fig 5.15 Objects which is used for sensor measurement

The response change is most likely to occur in a distance of 7mm and 1mm.The Fig 5.16 and Fig 5.17 depicts sensor response for different distances. The object used for checking is a steel cylinder of OD 13.5 mm.
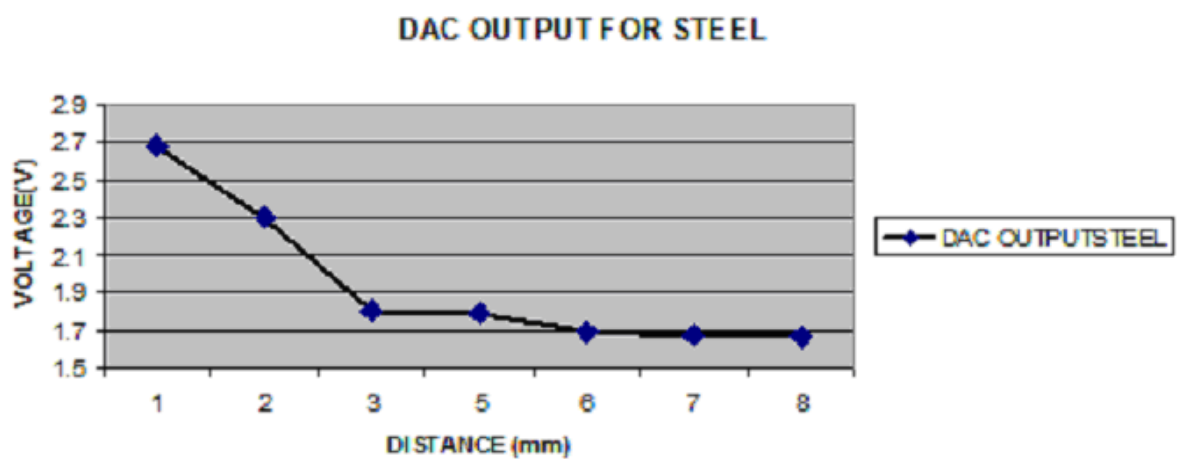

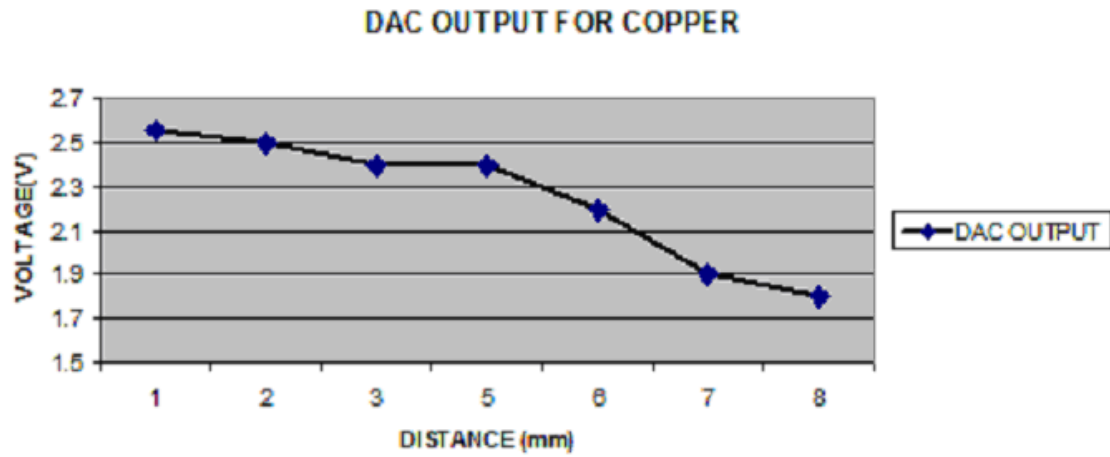Fig 5.16 DAC output for different distances to steel

DAC OUTPUT FOR COPPER

Fig 5.17 DAC output for different distances to copper

5.5 SENSOR RESPONSE IN PHANTOM

Metal detector magnetic field incident on the human body is also generating a small eddy current in the tissues. So the testing of the entire instrument with phantom material is relevant. A phantom constituting 3 gm of potassium Chloride (KCl) in 500 gm of de-ionised water [11] was prepared to emulate the tissue conductivity .The set up is shown in Fig 5.18. The readings were recorded for target at 5mm with and without phantom. It is given in Fig 5.19. From the graph, it is observed that the sensor is showing only 8mV change with phantom. The offset voltage with and without phantom is also depicted in Fig 5.20.The sensor is displaying only a change of 7mV in the offset voltage. The experimental setup of the sensor with phantom is shown in Fig 5.18
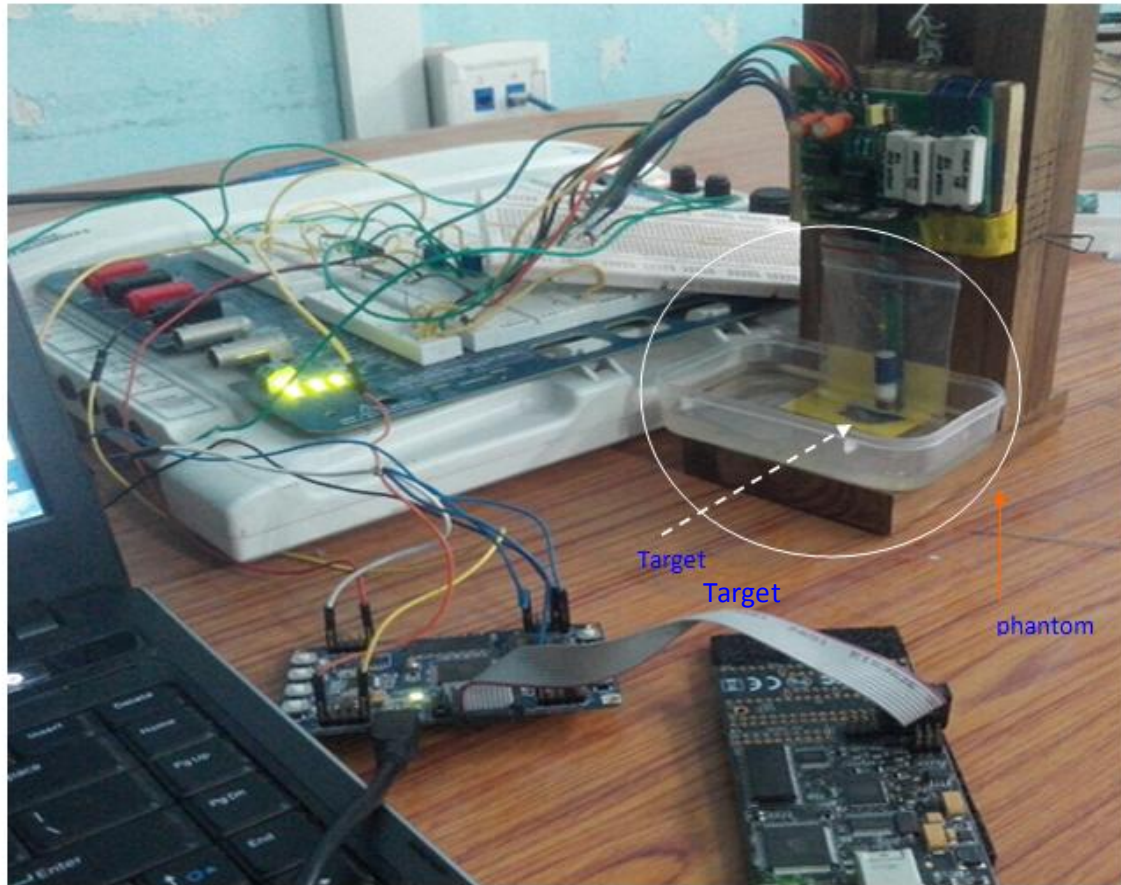
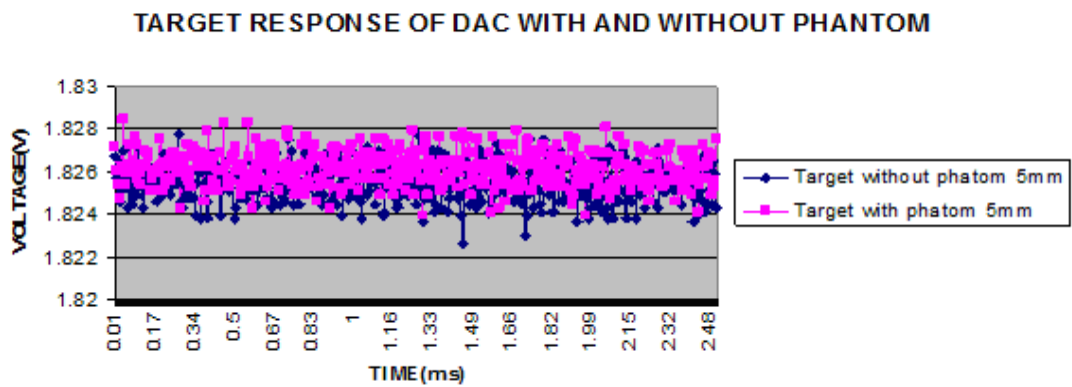Fig 5.18 Experimental setup of new IPS Sensor with Phantom

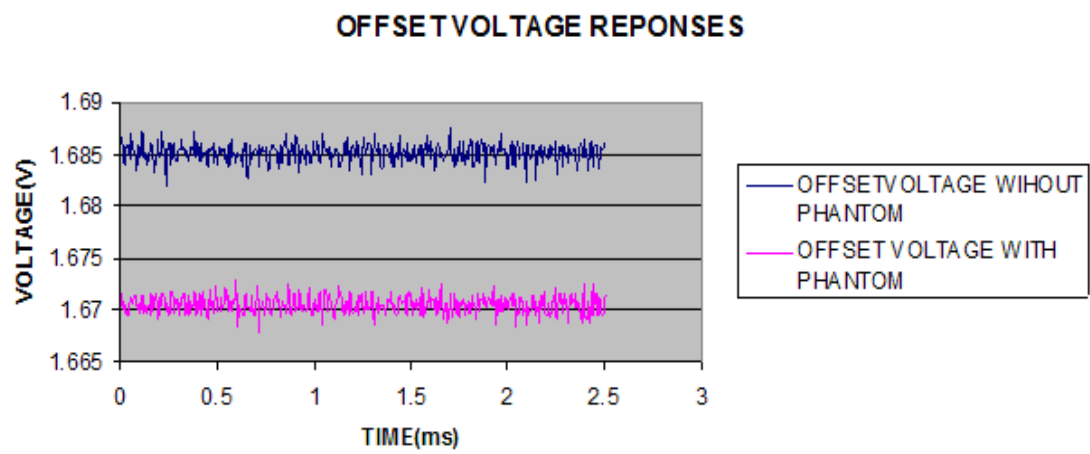Fig 5.19 DAC output for with and without Phantom for a target distance of 5mm

Fig 5.20 DAC output offset voltage response with and without Phantom

CHAPTER 6

CONCLUSION AND FUTURE SCOPE

6.1 CONCLUSION

In this project a microcontroller based portable metal shrapnel detector was developed. This work is based on a previous work done on an IPS (Inductive Proximity Sensor). By the use of microcontroller ATXMEGA 128A1 makes the system more compact and cost effective. The integrated 12-bit ADC acquires data from the sensor and used this data to modulate a base frequency of a 380 Hz. It requires only a 3.3 V battery to power the microcontroller. The speed of operation of the microcontroller can be increased by keeping the CPU frequency to 30MHz. The selection of this high frequency makes the ADC to run at its maximum sampling rate of 2MSPS. This allows the acquiring of maximum samples from the sensor output. The algorithm is based on simple peak detection algorithm, which makes the program simpler. The basic sensor has a new former design which is capable of eliminating the parasitic inductances. In this project, by using differential sensing method the detection depth of the sensor is increased. By keeping sensing coil and dummy coil in specially designed slot, which reduces the offset voltage produced due to the geometrical mismatch.

The electrical performance of the system has been measured. The system is checked with different materials like steel, copper and gold. By keeping the steel target, it's observed that the sensor is capable of giving a detection depth of 9mm and the target depth for copper is measured as 8mm. The system is tested for different shaped materials and the responses from each material is almost same. The instrument is also tested with

phantom .It is observed that, the change in the sensor output with phantom is insignificant.

6.2 FUTURE SCOPE

The sensor output contains so many frequency components. A moving average algorithm should be done before processing the sensor output by peak detection algorithm. It will help to smooth the sensor output. So we can get more noise free output.

REFERENCES

[1] J. Trevelyan, "Target depth estimation for a metal detector in the frequency domain," in *Proc. International conference on detection of abandoned land mines*, no. **458**, pp. 218–221, Oct. 1998.

[2] C. Xin, C. Kim, M. Pramanik, and L.V. Wang, "Photo-acoustic tomography of foreign bodies in soft biological tissue," *Biomedical Optics J.*, vol. **16**, no. **4**, pp. 046017-1 - 046017-4, Apr. 2011

[3] S. Jacob, T. Sella, D. Shaham, S.C. Shapira, A. Rivkind, A.I. Bloom, and E. Libson, "Faciing the new threats of terrorism: Radiologists' perspectives based on experience in Israel," in *Proc. Radiology*, vol. **237**, pp. 28–36, Oct. 2005.

[4] **M. Jagiella, S. Fericean, and A. Dorneich**, "Progress and Recent Realizations of Miniaturized Inductive Proximity Sensors for Automation," *IEEE Sensors J.*, vol. 6, no. 6, pp. 1734-1741, Dec. 2006.

[5] Victor F.Elia , "metal detector sensor –head using JMAG"*IEEE Trans. Instrum. Meas.*, vol. 58, pp. 3221-3231, Sep. 2009.

[6] M. Sakthivel, B. George, V. Jayashankar and M. Sivaprakasam, "A new inductive proximity sensor as a guiding tool for removing metal shrapnel during surgery," in *Proc. Instrumentation and Measurements Technology Conference (I2MTC)*, pp. 53–57, May. 2013

[7]www.atmel.com/xplained AVR 1924:XMEGA-A1 Xplained Hardware User's Revision 6/2013

[8] www.atmel.com/xplained 8/16 bit XMEGA A1 Revision 6/2013

[9] www.atmel.com/xplained Atmel AVR1300: Using the Atmel AVR XMEGA ADC Revision 6/2013

[10] www.atmel.com/xplained AVR 1301:Using the XMEGA DAC

[11] Gabriel, S Gabriely and E Corthout, "The dielectric properties of biological tissues: I. Literature survey", Phys. Med. Biol. **41** (1996) 2231–2249

[12] http://www.atmel.com/dyn/products/tools_card.asp?tool_id=4279 Atmel AVR Draggon

CURRICULUM VITAE

Name   : AMBILI A R

Date of Birth   : 05/05/1982

Place of Birth   : Velloorkunnam, Ernakulam, Kerala

B.Tech   : College of Engineering, Munnar, Kerala

Current Designation   : Working as Asst. Professor (NC) in

                                         FISAT Angamali, Kerala

Work Experience   : 6 years of Teaching Experience

Email   : ambucheer@yahoo.co.in